

OPEN ACCESS

Repository of the Max Delbrück Center for Molecular Medicine (MDC)
in the Helmholtz Association

<https://edoc.mdc-berlin.de/18368/>

DCAF8, a novel MuRF1 interaction partner, promotes muscle atrophy

Nowak M., Suenkel B., Porras P., Migotti R., Schmidt F., Kny M., Zhu X., Wanker E.E., Dittmar G., Fielitz J., Sommer T.

This is a copy of the final article, which is published here by [permission of the publisher](#) and which appeared first in:

Journal of Cell Science
2019 SEP 06 ; 132(17): jcs233395
doi: [10.1242/jcs.233395](https://doi.org/10.1242/jcs.233395)

Publisher: [The Company of Biologists Ltd](#)

Copyright © 2019 The Authors. Published by The Company of Biologists Ltd.

RESEARCH ARTICLE

DCAF8, a novel MuRF1 interaction partner, promotes muscle atrophy

Marcel Nowak^{1,2,*,#,††}, Benjamin Suenkel^{1,††}, Pablo Porras^{3,‡}, Rebekka Migotti^{4,§}, Franziska Schmidt^{2,¶}, Melanie Kny², Xiaoxi Zhu², Erich E. Wanker³, Gunnar Dittmar^{4,**}, Jens Fielitz^{2,5,6,§§} and Thomas Sommer^{1,7,8,§§}

ABSTRACT

The muscle-specific RING-finger protein MuRF1 (also known as TRIM63) constitutes a bona fide ubiquitin ligase that routes proteins like several different myosin heavy chain proteins (MyHC) to proteasomal degradation during muscle atrophy. In two unbiased screens, we identified DCAF8 as a new MuRF1-binding partner. MuRF1 physically interacts with DCAF8 and both proteins localize to overlapping structures in muscle cells. Importantly, similar to what is seen for MuRF1, DCAF8 levels increase during atrophy, and the downregulation of either protein substantially impedes muscle wasting and MyHC degradation in C2C12 myotubes, a model system for muscle differentiation and atrophy. DCAF proteins typically serve as substrate receptors for cullin 4-type (Cul4) ubiquitin ligases (CRL), and we demonstrate that DCAF8 and MuRF1 associate with the subunits of such a protein complex. Because genetic downregulation of DCAF8 and inhibition of cullin activity also impair myotube atrophy in C2C12 cells, our data imply that the DCAF8 promotes muscle wasting by targeting proteins like MyHC as an integral substrate receptor of a Cul4A-containing ring ubiquitin ligase complex (CRL4A).

This article has an associated First Person interview with the first author of the paper.

KEY WORDS: Atrophy, Cullin, MuRF1

INTRODUCTION

Muscle tissue represents the largest protein reservoir in the body that can be utilized as a source of amino acids for energy production during starvation. This so-called muscle atrophy involves the removal of contractile proteins like several different myosin heavy chain proteins (MyHC) by proteolytic systems, which in turn causes the reduction of the size of muscle fibers. The molecular details of muscle atrophy are of immanent medical importance because excessive loss of muscle mass counteracts the therapeutic treatment of cancer and other malignancies, aggravates the progression of most chronic diseases, prolongs the recovery phase after surgery, and increases overall morbidity and mortality. Proteolysis in muscles is mainly mediated by the ubiquitin-proteasome system (UPS). The UPS constitutes a cascade of E1 (ubiquitin-activating), E2 (ubiquitin-conjugating) and E3 (ubiquitin ligase) enzymes to attach ubiquitin onto substrate proteins, which initiates their degradation by 26S proteasomes. E3 ligases ensure the specificity of the UPS by selecting appropriate substrates and promoting the transfer of ubiquitin onto them. These components either act as individual enzymes or are organized in multi-subunit protein complexes (Hershko and Ciechanover, 1998; Buetow and Huang, 2016).

The ‘muscle-specific RING-finger’ proteins MuRF1, MuRF2 and MuRF3 (also known as TRIM63, TRIM55 and TRIM54, respectively) have been identified as important factors for the maintenance of protein homeostasis in muscle cells (Spencer et al., 2000; Foletta et al., 2011). However, the molecular function of MuRF1 is poorly understood and even less is known about MuRF2 and MuRF3. MuRF1 expression is highly upregulated during atrophy (Bodine et al., 2001), where it was reported to act as an autonomous ubiquitin ligase for the removal of proteins such as MyHC and actin (Clarke et al., 2007; Fielitz et al., 2007a; Cohen et al., 2009). Consistent with this, deletion of the MuRF1-encoding gene *Trim63* in mice or the reduction of MuRF1 levels in muscle cells through siRNA treatment inhibits muscle atrophy (Cohen et al., 2009; Castillero et al., 2013). MuRF1 was also found to localize to the sarcomere, to associate with titin and to stabilize the sarcomeric M-line (McElhinny et al., 2002; Gotthardt et al., 2003). Moreover, MuRF1 appears to regulate muscular energy metabolism by targeting creatine kinase (Hirner et al., 2008; Koyama et al., 2008). The large diversity of the published MuRF-associated activities suggests that these proteins team up with different co-factors, which integrate them into distinct cellular processes.

Through genetic and biochemical techniques we identified DDB1 and cullin-associated factor 8 (DCAF8), also termed WD repeat (WDR) containing protein 42A (WDR42A), as a new

¹Intracellular Proteolysis, Max Delbrück Center (MDC) for Molecular Medicine in the Helmholtz Association, Robert-Rössle-Strasse 10, 13125 Berlin-Buch, Germany.

²Experimental and Clinical Research Center (ECRC), Charité - Universitätsmedizin Berlin, MDC, Lindenberger Weg 80, 13125 Berlin-Buch, Germany. ³Proteomics and Molecular Mechanisms of Neurodegenerative Diseases, Max Delbrück Center (MDC) for Molecular Medicine in the Helmholtz Association, Robert-Rössle-Strasse 10, 13125 Berlin-Buch, Germany. ⁴Mass Spectrometric Core Unit, Max Delbrück Center (MDC) for Molecular Medicine in the Helmholtz Association, Robert-Rössle-Strasse 10, 13125 Berlin-Buch, Germany. ⁵Department of Internal Medicine B, Cardiology, University Medicine Greifswald, 17475 Greifswald, Germany. ⁶DZHK (German Center for Cardiovascular Research), Partner site Greifswald, Fleischmann Strasse 41, 17475 Greifswald, Germany. ⁷Institute of Biology, Humboldt-University Berlin, Invalidenstrasse 43, 10115 Berlin, Germany. ⁸DZHK (German Centre for Cardiovascular Research), Oudenarder Straße 16, 13347 Berlin, Germany.

*Present address: DUNN Labortechnik GmbH, Thelenberg 6, 53567 Asbach, Germany. †Present address: European Bioinformatics Institute (EMBL-EBI), European Molecular Biology Laboratory, Wellcome Genome Campus, Hinxton CB10 1SD, UK. ‡Present address: ProPharma Group, Siemensdamm 62, 13627 Berlin, Germany. ¶Present address: BCRT Flow and Mass Cytometry Lab, Charité - Universitätsmedizin Berlin, Augustenburger Platz 1, 13353 Berlin, Germany. **Present address: Proteome and Genome Research Laboratory, Luxembourg Institute of Health, 1a Rue Thomas Edison, L-1445 Strassen, Luxembourg.

††These authors contributed equally to this work

§§Authors for correspondence (jens.fielitz@uni-greifswald.de; tssommer@mdc-berlin.de)

© M.N., 0000-0002-0513-3254; B.S., 0000-0001-9774-4492; P.P., 0000-0002-8429-8793; R.M., 0000-0001-7183-1424; F.S., 0000-0001-7022-3531; X.Z., 0000-0001-7858-1114; E.E.W., 0000-0001-8072-1630; G.D., 0000-0003-3647-8623; T.S., 0000-0001-9990-5202

MuRF1 interaction partner. WDR proteins commonly serve as substrate receptors for cullin RING ligases (CRLs). These protein complexes represent modular E3 enzymes that are built around one of the seven cullin scaffolding proteins. Through their C-terminus, the cullins recruit specific RING-finger proteins involved in ubiquitin conjugation. Additional adaptor and receptor proteins that determine the specificity of the ubiquitylating reaction bind to their N-terminus. CRL4 complexes, for instance, encompass an appointed combination of the cullins Cul4A or Cul4B, the RING-finger proteins RBX1 or RBX2, DNA damage-binding protein 1 (DDB1), and an accessory DDB1- and CUL4-associated factor (DCAF) (Jackson and Xiong, 2009). It is noteworthy that CRL complexes seem to primarily be involved in the control of gene expression and in the regulation of the cell cycle (Petroski and Deshaies, 2005; Sarikas et al., 2011) and to contribute to lysosomal protein degradation (Lee et al., 2017) rather than to directly promote the proteasomal degradation of structural proteins like MyHC.

We demonstrate here that MuRF1 associates with a CRL4A multi-protein complex by binding to DDB1 and DCAF8. Similar to MuRF1, DCAF8 is strongly upregulated during denervation-induced skeletal muscle atrophy in mice. Moreover, we show that C2C12 skeletal muscle cells lacking DCAF8 resist glucocorticoid-induced myotube atrophy and that DCAF8 and MuRF1 directly participate in the UPS-dependent MyHC degradation. Since chemical inhibition of CRL activity impedes atrophy in our model system, we propose that a CRL4A ubiquitin ligase complex containing DCAF8 contributes to the proteasomal degradation of sarcomeric proteins like MyHC and thereby promotes muscle atrophy.

RESULTS

Identification of novel MuRF interaction partners

The multitude of the reported MuRF functions suggests that these proteins act in combination with yet unknown co-factors, which mediate the role of these RING finger proteins in diverse cellular functions. We thus performed two proteome-wide high-throughput (HT) screens to identify such binding partners. To this end, we employed automated unbiased yeast two-hybrid (Y2H) screens using a ~23,000 single-clone cDNA expression library as a prey and non-auto activating MuRF wild-type and truncation cDNA constructs as baits (Fig. 1A; Fig. S1, Table S1) (Fields and Song, 1989; Stelzl et al., 2005). In a second screen, we used stable isotope labeling by amino acids in cell culture (SILAC) and affinity purification (AP) of individual MuRF constructs, and analyzed the precipitates by mass spectrometry (MS). We transduced cDNAs encoding Myc(His)₆-tagged MuRF1, MuRF2, or MuRF3 by adenoviral vector (AdV) transfer into 'heavy' isotope-labeled H9c2 myocytes (lysine-8, arginine-10) and isolated the corresponding MuRF proteins by metal affinity purification. As a reference, we used 'light' isotope-labeled H9c2 myocytes (lysine-0, arginine-0) containing an empty vector [promoterless adenovirus (AdV-PL)] in the analysis (Fig. 1A, Fig. S2; Table S2).

The outputs of multiple screening rounds were scored (see Materials and Methods section) resulting in several putative MuRF-binding proteins (Tables S3–S12). Y2H employs plasmid-driven protein expression of bait (MuRF1–MuRF3) and prey (~23,000 single-clone cDNA expression library, see above) constructs in the heterologous organism *S. cerevisiae*. Positive hits in this screening method do not necessarily represent partner proteins, since the candidates may not even be expressed in the same tissue in mammals. Similarly, the SILAC-AP-MS approach employs overexpressed and epitope-tagged MuRF proteins and this may result in the identification of factors that unspecifically and only

weakly interact with the unnatural high amounts of the bait. Thus, we first validated our findings by comparing the hits of both experiments. In the end, 43 candidate proteins were considered to be enriched in both the SILAC-MS and the Y2H assays (Fig. 1A; Table S13). Importantly, the identification of already-known MuRF substrates and interacting proteins underscored the reliability of both screening approaches. Among others, we isolated the sarcomeric proteins nebulin and FHL-1, which have been shown to associate with the MuRF proteins, the MuRF substrates titin-cap/telethonin and troponin, and proteins linked to the UPS and autophagy such as UBE2I, USP13, UCHL3, ubiquitin and Sqstm-1 (also known as p62) (McElhinny et al., 2002; Kedar et al., 2004; Lange, 2005; Witt et al., 2005; Fielitz et al., 2007b; Hirner et al., 2008; Loch and Strickler, 2012; Woodsmith et al., 2012).

We then validated the results from the HT screens further in individual immunoprecipitation (IP) reactions (selected validated interactors are summarized in Fig. 1B). FLAG-tagged candidate proteins were co-expressed with Myc(His)₆-tagged MuRF proteins in COS-7 cells under the control of the same promoter to yield near-stoichiometric cellular protein levels, immunopurified from cell extracts, and the precipitates were analyzed by immunoblotting with anti-Myc and anti-FLAG antibodies. Importantly, we were able to reproduce published data for the binding of established MuRF partner proteins in these assays (Fig. 1C,D; Fig. S3). For instance, the selective autophagy receptor protein Sqstm1 was shown to interact with MuRF1 (Khan et al., 2014; Troncoso et al., 2014) and indeed the FLAG-tagged isoform 1 of Sqstm1 efficiently precipitated MuRF1–Myc(His)₆ in our experiments (Fig. 1C). Interestingly, MuRF1 was not purified with Sqstm1 isoform 2, which lacks 84 amino acids at its N-terminus, implying that the N-terminal region of isoform 1 confers binding to MuRF1 (Fig. 1C). Similarly, USP13 was described to specifically bind MuRF1 and MuRF2, but not MuRF3 (McElhinny et al., 2002), which matches the results of our IP experiments (Fig. S3A,D,E).

We then investigated binding of new putative MuRF interaction partners in the IP assay. For some of the high scoring hits of the HT screens, like the AAA-ATPase p97 (also known as VCP), we were not able to confirm a physical interaction with the corresponding MuRF protein in these experiments (Fig. S3A,D; Table S14). However, FLAG-tagged variants of 14 of the tested HT candidates precipitated at least one MuRF construct (Fig. 1C,D; Fig. S3, Table S14). Surprisingly, only one of these, the myosin light chain kinase 2 (MYLK2) has been reported to be preferentially expressed in muscle tissue (UniProt database, entry Q9H1R3). MYLK2–FLAG precipitated all three MuRF–Myc variants when co-expressed in COS-7 cells, but the biological significance of this observation was not pursued further (Fig. 1D).

Remarkably, we observed binding of several components of the UPS, such as the ubiquitin conjugating enzyme UBE2E3, the ubiquitin specific proteases USP13 and USP35, the F-Box and WD repeat containing protein FBXW2, the regulator of cullin-type ubiquitin ligases NEDD8, and the WD repeat containing protein DCAF8 to at least one MuRF protein (Fig. 1C; Fig. S3, Table S14). Of these, DCAF8 caught our particular attention. In the IP experiments, DCAF8–FLAG specifically precipitated MuRF1 and MuRF3 (Fig. 1D). Importantly, DCAF8 was previously linked to the regulation of muscle mass since mutations in the coding gene that impair the interaction of the protein with DDB1 are associated with the development of axonal hereditary motor and sensory neuropathy (HMSN2), which leads to a progressive muscular atrophy of the extremities (Klein et al., 2014). DCAF8 also contains so-called WD repeat domains and has been reported to constitute a bona fide substrate recruiting factor of cullin RING ligase 4- (CRL4-)

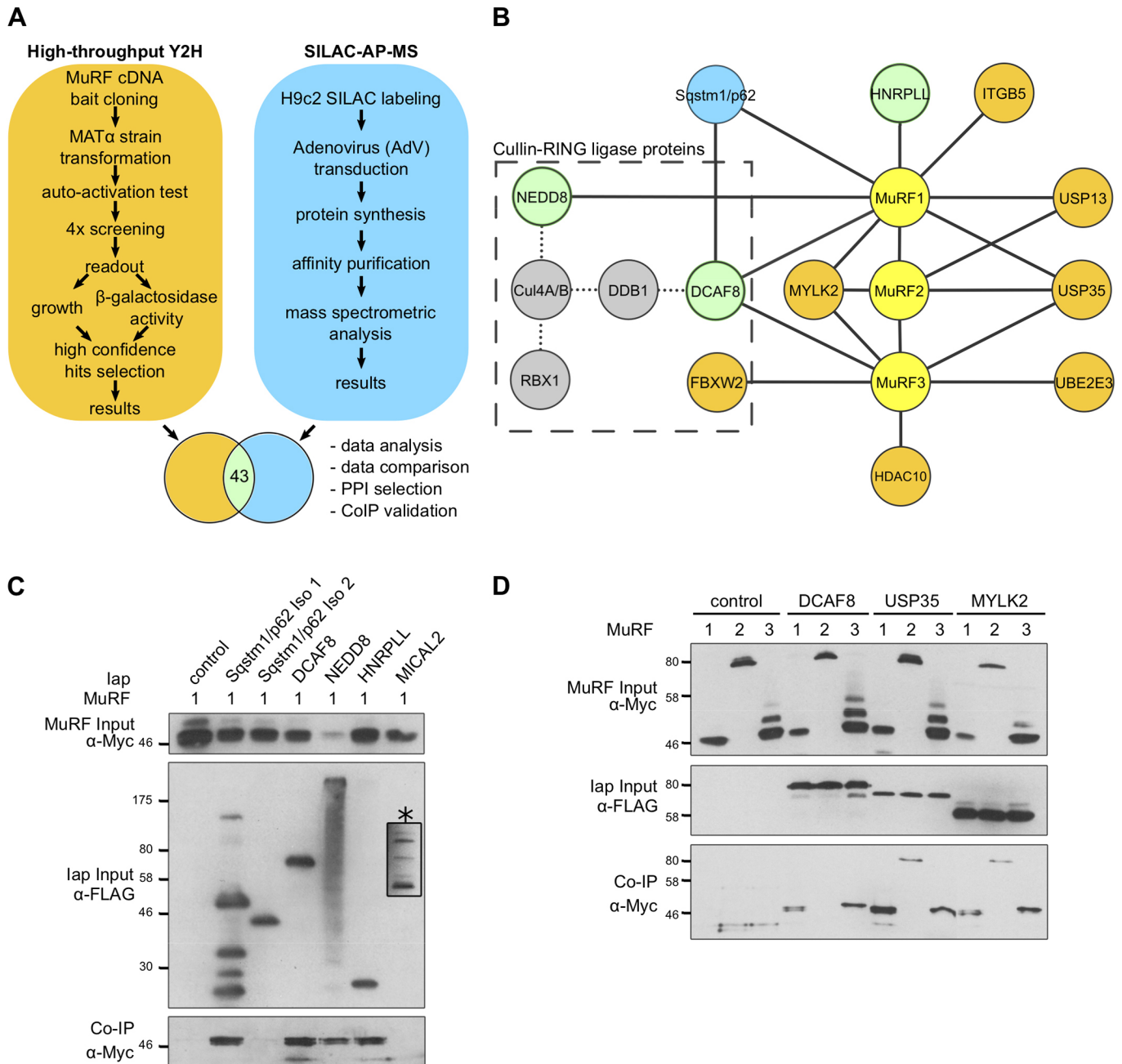


Fig. 1. MuRF1 and MuRF3 specifically interact with DCAF8. (A) Graphical representation of the experimental workflow of the Y2H and SILAC-AP-MS high-throughput screens; 43 putative MuRF interaction partners were identified in both approaches. (B) Overview of selected validated protein interactions. Hits from initial screenings are colored in orange (Y2H), blue (SILAC-AP-MS) or green (identified with both screening methods), whereas interaction partners published in other works but not identified in our screens are labeled as gray dotted lines. (C,D) Interaction validation by co-IP experiments after transient co-expression of FLAG fusions of potential new MuRF-binding partners (denoted as lap; interaction partner) and Myc(His)₆-tagged MuRF proteins in COS-7 cells. 14 candidates precipitated individual MuRF proteins, indicating a physiological interaction (see Fig. S3 and Table S14 for a complete list of validated interaction partners). Asterisk and inset indicates longer exposure of the MICAL2-FLAG immunoblot.

type ubiquitin ligase complexes (Jin et al., 2006). Aside from the cullin regulator NEDD8, DCAF8 was therefore another CRL4 component that was enriched in our screens (Fig. 1B).

DCAF8 is a stable MuRF1 interaction partner

We subsequently investigated whether DCAF8 constitutes a functional interaction partner of the MuRF proteins or represents a substrate of these putative ubiquitin ligases. Thus, we determined the half-life of DCAF8 and the MuRF proteins in transiently transfected COS-7 cells. In short, cells were treated with cycloheximide (CHX) to

block the synthesis of new polypeptides and time-dependent changes of the amount of selected proteins were recorded by immunoblotting. In these assays all MuRF-Myc(His)₆ proteins and FLAG-tagged DCAF8 were stable for 4 h (Fig. 2A). FLAG-tagged DCAF8 that was expressed with any of the MuRF-Myc(His)₆ proteins displayed no significant change in stability. Likewise, all MuRF proteins were stable when DCAF8 was co-expressed indicating that DCAF8 does not initiate their turnover and vice versa (Fig. 2B). In line with these findings the half-life of endogenous DCAF8 in COS-7 cells was also unaffected by increased MuRF1 levels (Fig. 2C). Hence, DCAF8

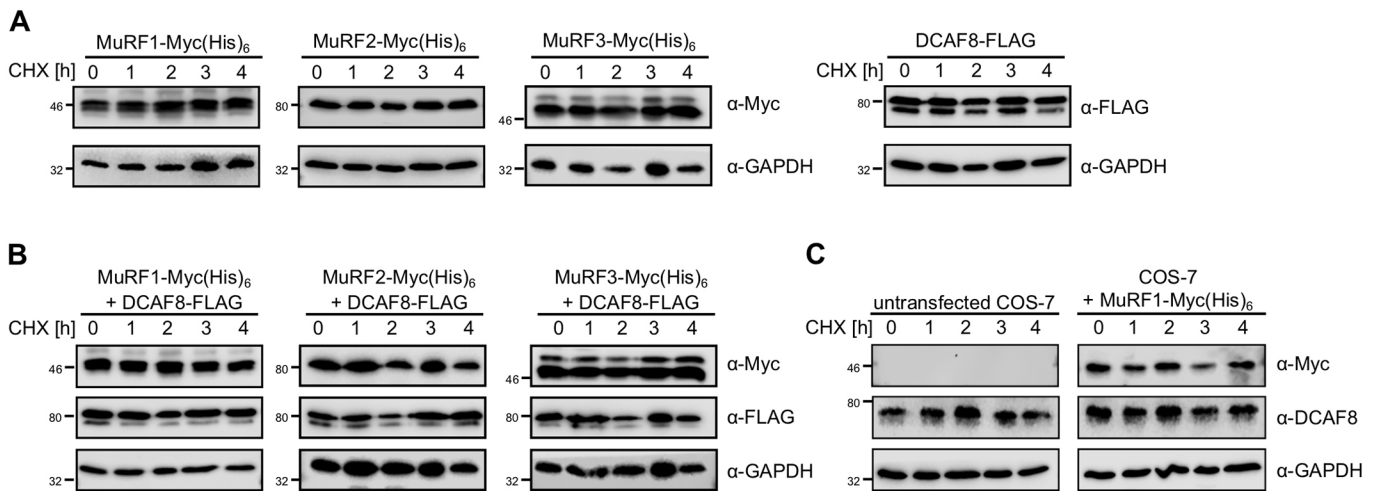


Fig. 2. Protein stability of DCAF8 and MuRF1 expressed in COS-7 cells. (A,B) Constructs for the expression of MuRF–Myc(His)₆ and/or DCAF8–FLAG were transfected into COS-7 cells and the stability of these proteins was determined in cycloheximide (CHX) decay assays followed by immunoblotting using the indicated antibodies. (C) MuRF1–Myc(His)₆ was expressed in COS-7 cells and changes in the amounts of endogenous DCAF8 were recorded after the addition of CHX by immunoblotting with the antibodies indicated. Immunoblots showing the amount of GAPDH in the samples serve as loading controls. Numbers refer to the time in hours after the addition of CHX.

seems not to be degraded in a MuRF1-dependent manner but rather represents a stable binding partner of this RING-finger protein.

MuRF1 and DCAF8 localize to overlapping cellular structures in muscle cells

As MuRF1 solely resides in striated muscle tissue, such as skeletal muscle and the heart (Bodine et al., 2001), we were interested in the expression pattern of DCAF8. A polyclonal DCAF8 antibody reacted with proteins displaying an apparent molecular mass of ~70 kDa in immunoblots of lysates from of COS-7 cells (Fig. 2C) and C2C12 myoblasts (Fig. 3A), which roughly matches the calculated molecular mass of the DCAF8 protein of ~67 kDa. Interestingly, in C2C12 cells, another DCAF8 species was observed at 80 kDa, which appeared to be more prevalent and may represent phosphorylated DCAF8 (five putative phosphorylation sites are annotated for DCAF8 in the UniProt database, entry Q8N7N5). Both signals were not detected in cells treated with DCAF8-specific siRNAs. Using this antibody, we observed, in immunoblots of mouse tissue samples, comparable levels of DCAF8 in the *Gastrocnemius plantaris* (GP) and *Tibialis anterior* (TA) skeletal muscle, in the heart and in other organs (Fig. 3B). Analogous to what was found for the C2C12 cell lysate, DCAF8 was detected as a doublet with molecular masses of 70 and 80 kDa in the majority of these tissues, but their relative abundance varied. Whether these signals and other species, of 35 kDa and 50 kDa, respectively, recorded in pancreas, liver and kidney lysates derive from posttranslational modifications, or limited proteolysis remains to be determined. Notably, the UniProt database lists several entries for truncated human, mouse and even claw frog DCAF8. Thus, the polyclonal antibody may react with different and tissue-specific isoforms of DCAF8.

We next analyzed the intracellular localization of MuRF1 and DCAF8. As determined by fluorescence microscopy, RFP and GFP fusion proteins of DCAF8 and MuRF1, respectively, resided as granules within the cytosol of COS-7 cells (Fig. 3C). Importantly, the majority of both constructs stained overlapping structures in these cells. Likewise, immunostaining of fixed undifferentiated and differentiated C2C12 cells with specific anti-MuRF1 or anti-DCAF8 antibodies (see below) revealed that endogenous DCAF8 and MuRF1 were excluded from the nucleus and localized in the cytosol (Fig. 3D). Still, we noticed

that in COS-7 and in C2C12 cells a fraction of the MuRF1 staining did not overlap with the DCAF8 signal and vice versa, which suggests that both proteins also associate with other partners.

MuRF1-bound DCAF8 still associates into a CRL4 ubiquitin ligase complex

DCAF8 has been proposed to serve as substrate receptor in CRL4 complexes in non-muscle cells (Jin et al., 2006; Li et al., 2017). Such modular E3 ligases usually contain a Cul4A or Cul4B cullin scaffolding protein, which recruits the RING-finger protein RBX1 or RBX2, the adaptor protein DDB1, and different DCAF proteins involved in substrate binding (Angers et al., 2006). To test whether DCAF8 bound to MuRF1 was still part of such a CRL4 ubiquitin ligase or whether MuRF1 binding sequesters DCAF8 from such cullin complexes, we performed FLAG-IP experiments from COS-7 cells that transiently overexpressed combinations of epitope-tagged variants of MuRF1, DCAF8 and DDB1. As expected from our previous experiments, we purified MuRF1–Myc(His)₆ with DCAF8–FLAG, indicative of a physical interaction (Fig. 4A). Of note, cells transfected with constructs for the expression of epitope-tagged MuRF1 contained higher amounts of this protein than ones harboring additional plasmids encoding DCAF8–FLAG or other proteins (Fig. 4D,E). We made a similar observation when we analyzed cells transfected for the overexpression of epitope-tagged DCAF8 (Fig. 4C) or DDB1 (Fig. 4E). For the following reasons, this effect most likely originates from the transfection procedure and does not implicate enhanced degradation of MuRF1, DCAF8 and/or DDB1. First, we noticed a decrease in the content of any epitope-tagged protein in cells that were co-transfected with another construct irrespective of the encoded gene (Fig. 4D,E). Second, we observed that the overexpression of DCAF8 did not change the stability of the MuRF1 protein in COS-7 cells (Fig. 2B) nor did overexpression of MuRF1 affect the amount of endogenous DCAF8 in COS-7 cells (Fig. 2C). Finally, a stable knockout of DCAF8 in C2C12 myocytes did not contain increased protein levels of DDB1 or DCAF8 (see below, Fig. 5C). We also detected DCAF8–FLAG in precipitates of DDB1–HA and retrieved DDB1–FLAG upon purification of DCAF8–Myc(His)₆ (Fig. 4B,C), which is in agreement with published data (Li et al., 2017). Interestingly, we

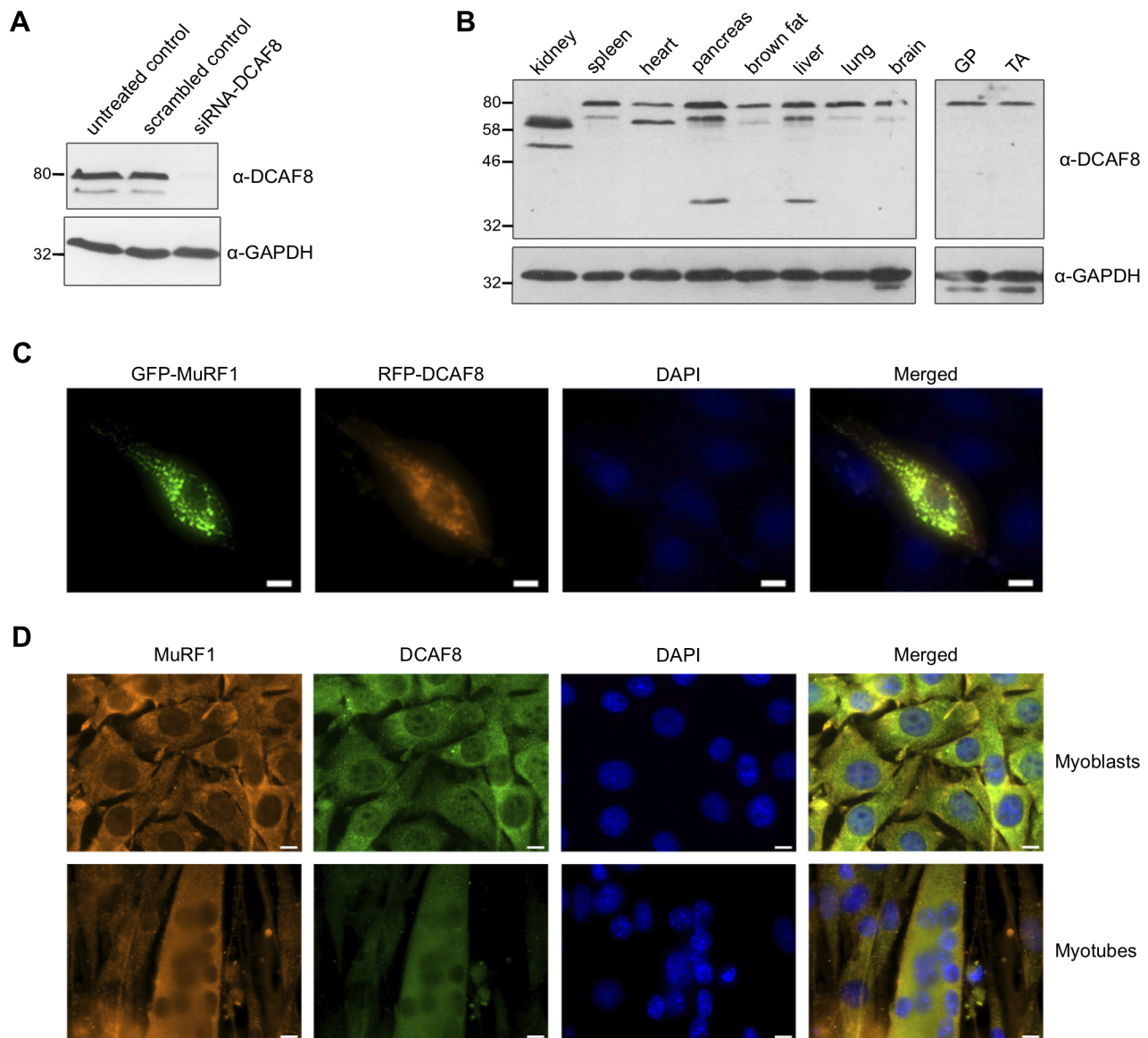


Fig. 3. DCAF8 is ubiquitously expressed and localizes to similar cellular structures to MuRF1 in myocytes. (A) C2C12 cell lysates were analyzed by immunoblotting with polyclonal anti-DCAF8 antibodies. Where indicated, the cells were treated with DCAF8-specific siRNA before lysate preparation. (B) Immunoblot of mouse tissue samples using the polyclonal anti-DCAF8 antibody. GP, *Gastrocnemius plantaris*, TA, *Tibialis anterior*. Immunoblots using an anti-GAPDH antibody serve as loading controls. (C) C2C12 myoblasts co-transfected with constructs for the expression of GFP–MuRF1 and RFP–DCAF8 were grown for 48 h and analyzed by fluorescence microscopy. (D) C2C12 myoblasts and myotubes were fixed with paraformaldehyde and stained with polyclonal antibodies against MuRF1 and DCAF8 and appropriate secondary antibodies. Scale bars: 10 μ m.

found MuRF1–Myc(His)₆ in precipitates of DDB1–FLAG (Fig. 4D). Since we also co-purified epitope-tagged MuRF1 and DDB1 with DCAF8–FLAG, our findings suggest that these three proteins form a complex (Fig. 4E). To analyze this idea in more detail, we downregulated DCAF8 with siRNA in COS-7 cells and isolated DDB1–FLAG. Even in absence of DCAF8 we co-precipitated MuRF1–Myc(His)₆ with DDB1–FLAG (Fig. 4F).

Next, we employed antibodies specific for DCAF8 or DDB1 in IPs from C2C12 myotube lysates to confirm complex formation of the endogenous proteins. Intriguingly, in precipitates using a polyclonal anti-DCAF8 antibody we found DDB1, Cul4A, RBX1 and, most importantly, also MuRF1 (Fig. 5A). We conducted a similar experiment using a polyclonal anti-DDB1 antibody. Again, we co-precipitated the components of a CRL4A complex, Cul4A, DCAF8, RBX1 and MuRF1, along with DDB1 from C2C12 myotube lysates (Fig. 5B).

These results indicate that DCAF8 is part of a cullin-type ligase in myocytes, even when bound to MuRF1. Given that DCAF proteins associate with CRL4 complexes via binding to DDB1 we wondered, whether MuRF1 also interacts with this adaptor protein. Therefore, we established a stable C2C12 cell line lacking DCAF8 using CRISPR/Cas9 (Fig. S4C). Strikingly, even in absence of endogenous DCAF8, we still detected MuRF1 in precipitates of DDB1 (Fig. 5C), which agrees with the knockdown co-IP results in COS-7 cells (Fig. 4F). Taken together, these results imply that MuRF1 interacts with CRL4A complexes in myocytes via direct binding to DDB1 and DCAF8.

DCAF8 levels increase during myocyte differentiation and denervation-induced skeletal muscle atrophy

So far, we have been able to show a physical interaction of MuRF1 with DCAF8 and a CRL4A-type ubiquitin ligase, but up to now a

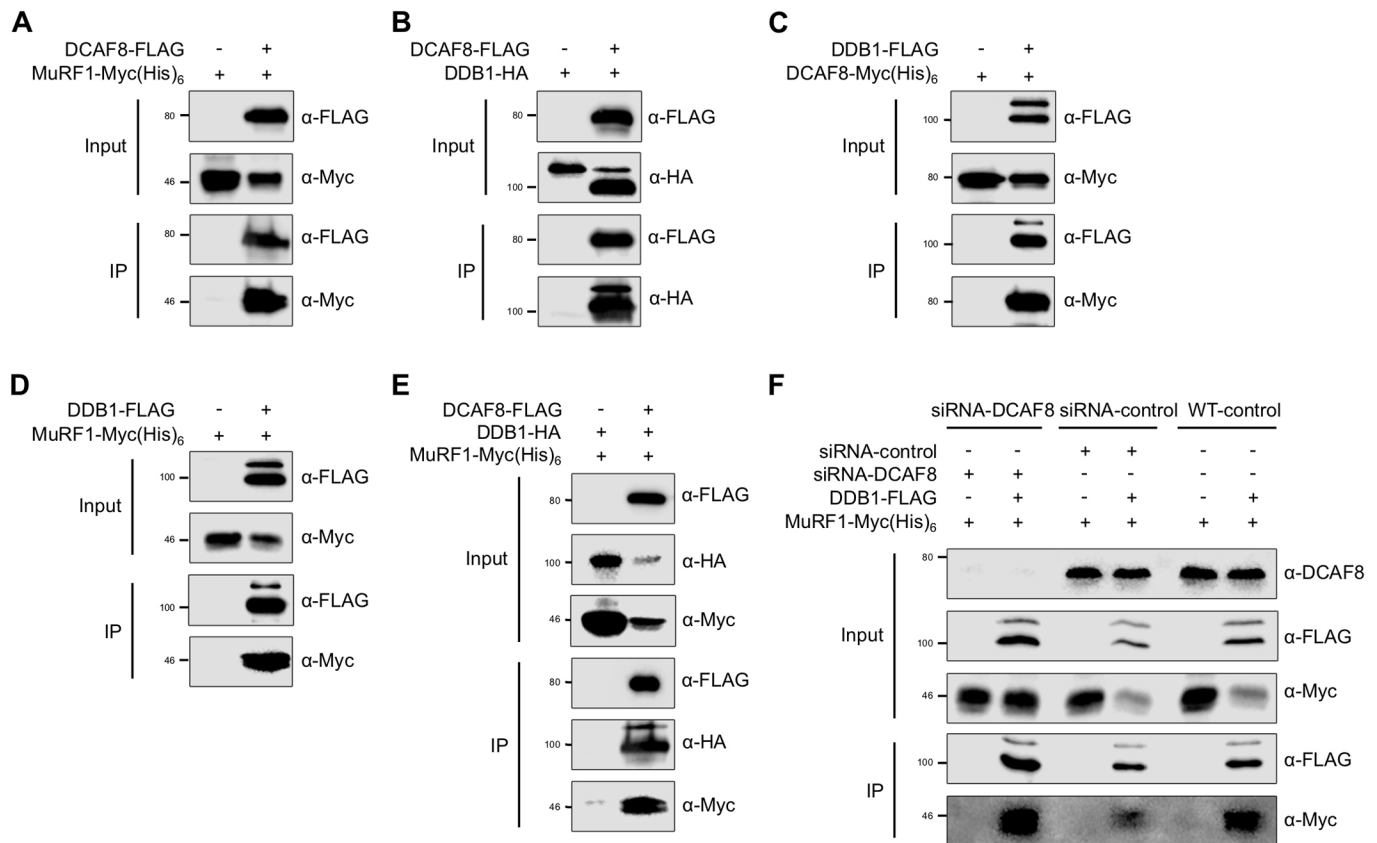


Fig. 4. Epitope-tagged variants of MuRF1, DCAF8 and DDB1 co-precipitate in COS-7 cells. (A–E) Cells expressing the indicated combinations of epitope-tagged MuRF1, DCAF8 and DDB1 were lysed, FLAG-tagged proteins were purified and the precipitates were analyzed by immunoblotting using the indicated antibodies. (F) Where indicated, endogenous DCAF8 was knocked down by siRNA in COS-7 cells, DDB1-FLAG was isolated, and the precipitates analyzed by immunoblotting with the respective antibodies.

specific function of such a complex in myocytes has not been described. MuRF protein levels change substantially during development and myogenic differentiation of C212 cells (Centner et al., 2001; Perera et al., 2012) and we wanted to determine whether the cellular content of its interaction partner(s) are regulated in a similar manner. Thus, we differentiated C2C12 myoblasts into myotubes by reducing the amount of serum in the medium for 4 days and monitored the levels of Cul4A, RBX1, DDB1, DCAF8 and MuRF1 by immunoblotting (Fig. 6A,B). Throughout differentiation we observed a moderate increase in the cellular content of DDB1 and a more pronounced rise in the amounts of Cul4A and DCAF8. Intriguingly, we also detected a substantial augmentation of MuRF1 and RBX1 protein levels. This finding correlates with published results on MuRF1 expression (Centner et al., 2001; Perera et al., 2012) and with the reported involvement of CRL-type ligase complexes, which contain RBX1, in myocyte differentiation (Blondelle et al., 2017).

Because the amount of MuRF1 strongly increases in atrophic muscle (Bodine et al., 2001; Foletta et al., 2011), we investigated whether DCAF8 expression is also upregulated during this process. We induced muscle atrophy in mice by denervation of the sciatic nerve (Schmidt et al., 2014) and determined the amount of DCAF8 by immunoblotting. Compared to sham operated mice, denervation led to a significant decrease in the mass of TA and GP muscles after 7, 14 and 21 days of surgery (Schmidt et al., 2014). Strikingly, we observed a significant increase of DCAF8 protein content in denervated TA and GP muscle tissue compared to innervated muscles in three individual animals (Fig. 6C–F; Fig. S5). These results

demonstrate that DCAF8 levels in muscle cells significantly increase during differentiation and atrophy, which correlates with increased expression of MuRF1 during atrophy.

DCAF8 is required for MyHC degradation

MuRF1 was shown to facilitate the ubiquitylation of MyHC, a highly abundant muscle protein, which is degraded during atrophy (Fielitz et al., 2007a). The upregulation of DCAF8 during atrophy prompted us to investigate whether this protein is also involved in MyHC proteolysis. To this end, we employed COS-7 cells, which endogenously express DCAF8 (see Fig. 2C) and the core components of CRL4A-type ligase complexes, and analyzed the turnover of transiently expressed FLAG-tagged MyHC (FLAG-MyH7) in CHX decay assays (see above). As a control we transfected a construct for the expression of FLAG-tagged Cas9, which is unrelated to the UPS. Importantly, the FLAG-MyHC protein level decreased by 30% after 30 min of CHX treatment in wild-type (WT) cells while it remained unchanged in COS-7 cells lacking DCAF8 (COS-7 Δ DCAF8; Fig. 7A,B; Table S15). Importantly, expression of DCAF8-FLAG in COS-7 Δ DCAF8 cells restored the turnover of co-transfected FLAG-MyHC ($39.0 \pm 6.1\%$ decrease, mean \pm s.e.m.; Fig. 7A,B; Table S15). Likewise, the expression of MuRF1-Myc(His)₆ in COS-7 Δ DCAF8 cells also induced FLAG-MyHC degradation to some extent ($22.5 \pm 5.3\%$ decrease after 30 min). These data imply that DCAF8 as well as MuRF1 contribute to the degradation of MyHC in COS-7 cells.

Subsequently, we recorded the steady state levels of FLAG-MyHC by immunoblotting in COS-7 cells that transiently

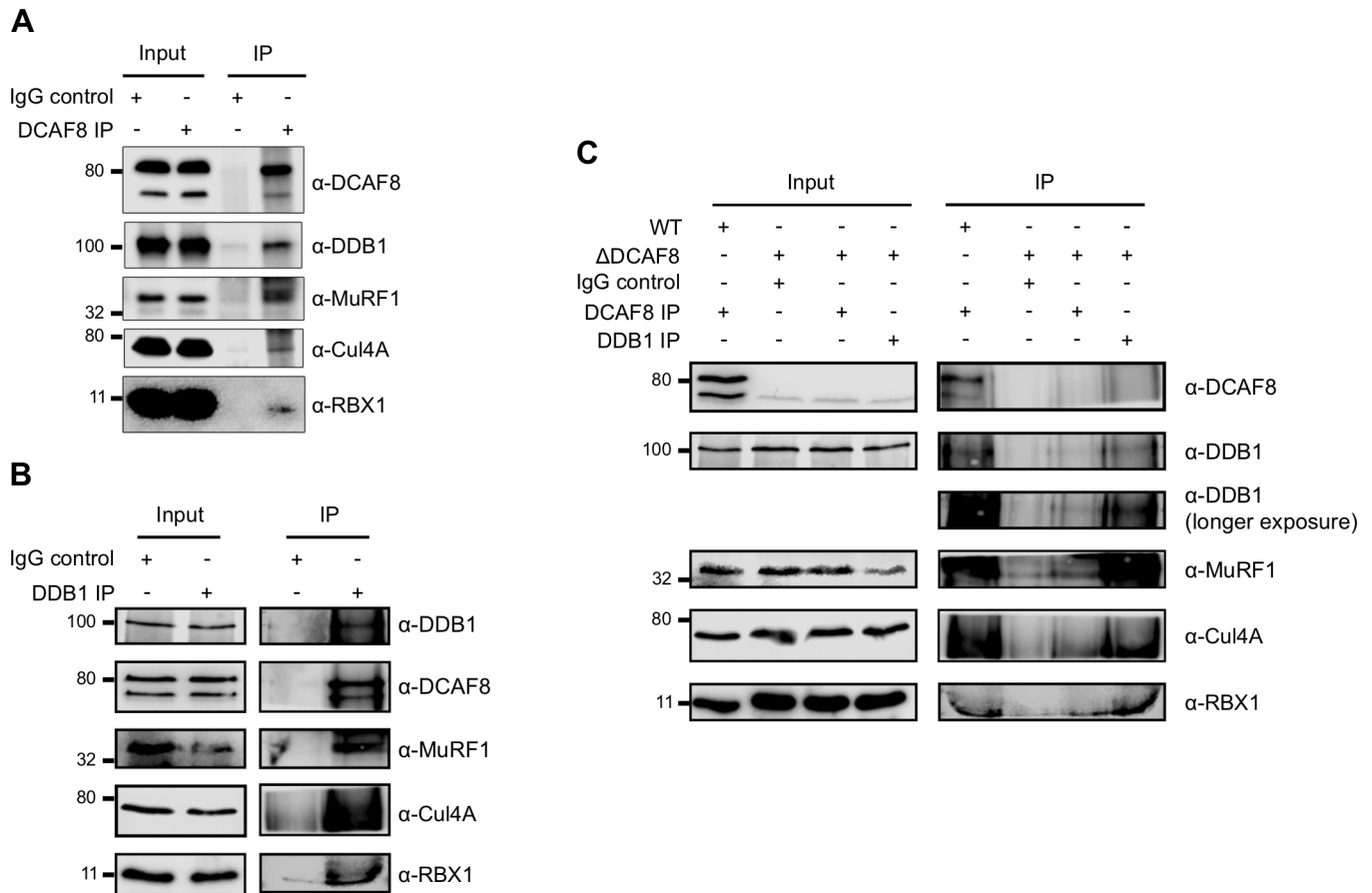


Fig. 5. Endogenous MuRF1 interacts via DCAF8 and DDB1 with CRL4 complex components. Endogenous DCAF8 (A) or DDB1 (B) were isolated from lysates of differentiated C2C12 cells using specific antibodies and the precipitates were analyzed by immunoblotting with the indicated antibodies. (C) DCAF8 or DDB1 were isolated from C2C12 myotubes or C2C12 ΔDCAF8 myotubes and samples were probed for the respective proteins by immunoblotting.

co-expressed either FLAG-tagged Cas9 or MuRF1–Myc(His)₆. Compared to Cas9-transfected cells, we observed an 80% reduction of the FLAG–MyHC protein amount in COS-7 cells harboring the MuRF1 construct. Treatment of these cells with MLN4924, which prevents the neddylation of CRL-type ubiquitin ligases and thereby impedes their activity (Blondelle et al., 2017), or the proteasomal inhibitor lactacystin restored the FLAG–MyHC content to WT levels. This observation confirms an involvement of CRL-type ligases and the proteasome in the degradation of FLAG–MyHC (Fig. 7C,D).

In COS-7 ΔDCAF8 cells we found an ~2-fold increase in the FLAG–MyHC protein content compared to COS-7 WT cells (Fig. 7C,D; Table S16). Expression of either MuRF1–Myc(His)₆ or DCAF8–FLAG in these cells restored the MyHC levels to that detected in COS-7 WT cells (Fig. 7C,D; Table S16). As expected, transfection of COS-7 ΔDCAF8 cells with both the DCAF8–FLAG and MuRF1–Myc(His)₆ constructs yielded a similar low MyHC protein content as in COS-7 WT transfected with MuRF1 (Fig. 7C,D). The addition of MLN4924 or lactacystin to these cells substantially increased the amount of FLAG–MyHC (Fig. 7C,D). Taken together, the experiments in the heterologous COS-7 cells show that MuRF1 and DCAF8 on their own are capable of facilitating the turnover of MyHC and that both proteins display additive effects in the degradation of MyHC. However, the functional relation between MuRF1 and DCAF8 in COS-7 cells remained unclear.

We therefore sought to validate our observations in C2C12 cells, which represent a more physiologically relevant system to study muscle-specific activities. To this end, we differentiated C2C12 cells that were downregulated for expression of individual genes into myotubes and induced atrophy using the glucocorticoid dexamethasone (Dexa). Dexa treatment serves as an established method to investigate muscle atrophy in cell culture but widely different concentrations of this substance have been used in individual studies (Hasselgren, 1999; Clarke et al., 2007; Menconi et al., 2008; Massaccesi et al., 2016). In initial experiments we exposed the C2C12 myotubes to 10 μM Dexa (defined as a ‘mild Dexa treatment’) and, as recently published, this treatment caused a decrease in MyHC protein levels in scrambled siRNA-treated control cells (Fig. 8A) (Massaccesi et al., 2016). In cells impeded for the expression of either MuRF1 or DCAF8 the loss of MyHC was less pronounced. The combined downregulation of MuRF1 and DCAF8 had a similar impact on the MyHC protein as the single knockdowns, implying that both proteins act in the same pathway for MyHC reduction. Because the atrophic response in the control cells was rather weak and the results in the single DCAF8 knockdown samples showed large deviations, we repeated this experiment with the C2C12 ΔDCAF8 cell line (Fig. S4) and treated the cells after differentiation with 100 μM Dexa (defined as a ‘strong Dexa treatment’) (Clarke et al., 2007). Again, we observed a substantial decrease in the amount of MyHC after Dexa treatment in WT myotubes but not in DCAF8-knockout cells (Fig. 8B).

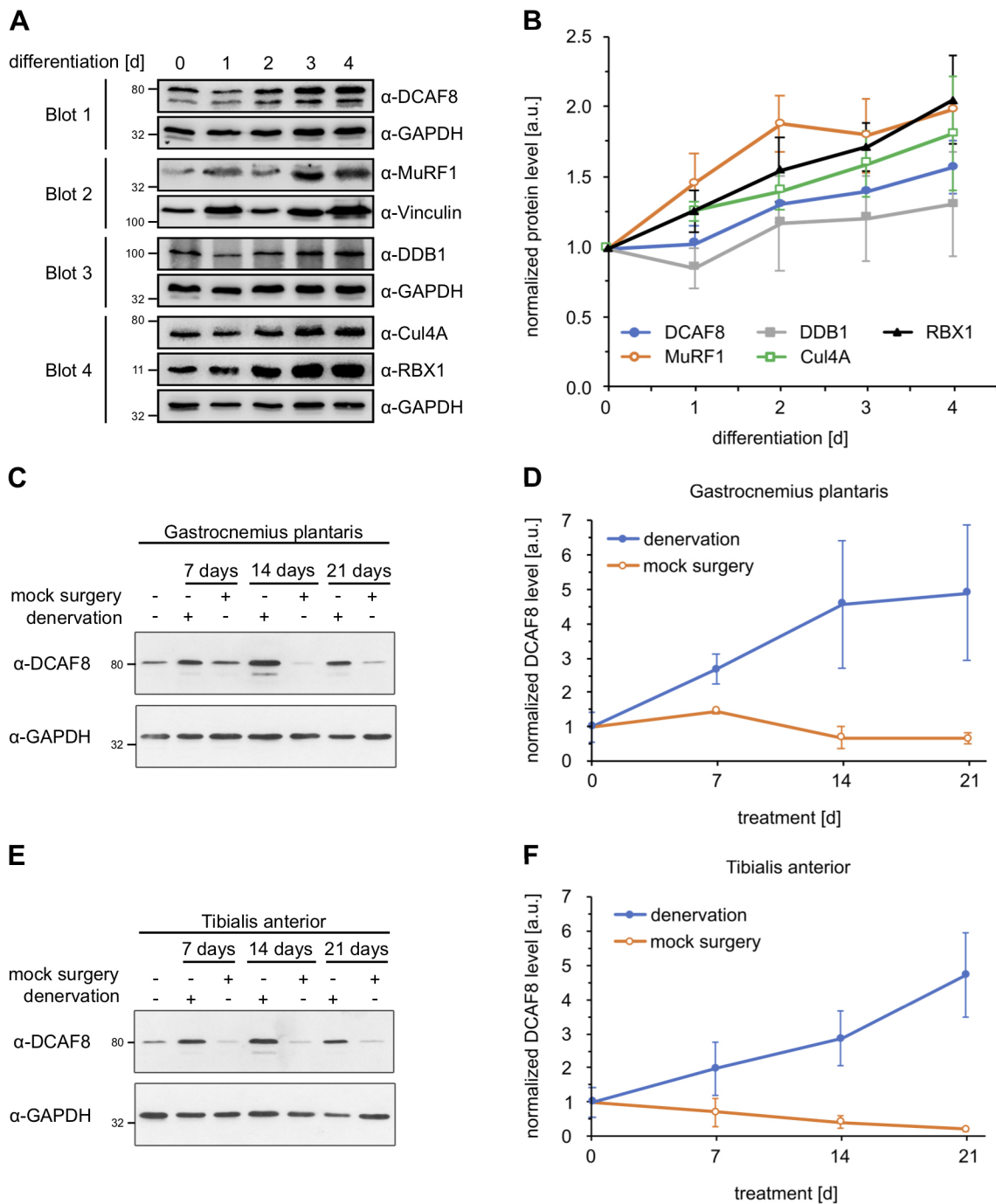


Fig. 6. DCAF8 is enriched in differentiating C2C12 myocytes and atrophic muscle tissue. (A,B) C2C12 myoblasts were differentiated into myotubes by reducing the amount of serum in the medium, and samples were taken at the indicated time points during this process. The amount of the indicated proteins was then determined by immunoblotting (a representative blot of three independent experiments is shown). Signals were quantified and normalized to the loading control GAPDH. (C–F) Denervation-induced skeletal muscle atrophy after dissection of the left sciatic nerve of C57BL/6N mice for 7, 14 and 21 days. Proteins were extracted from *Gastrocnemius plantaris* and *Tibialis anterior* muscles and the amount of the DCAF8 protein levels determined by immunoblotting. Immunoblots using an anti-GAPDH antibody serve as loading controls. A representative blot of three independent experiments is shown (see also Fig. S5). a.u., arbitrary units.

MyHC levels remained largely unchanged, when cells were exposed to Dexamethasone and the neddylation inhibitor MLN4924 or the proteasomal inhibitor MG132 in this assay. Other than in the COS-7 experiments (see above), where MyHC turnover was already strongly induced in presence of either DCAF8 or MuRF1 alone, the results from C2C12 myocytes imply that the degradation of MyHC during atrophy relies on MuRF1 as well

as on DCAF8, and involves the activity of CRL-type E3 ubiquitin ligase complexes and the proteasome.

C2C12 myotubes lacking DCAF8 are resistant to atrophy

Given the upregulation of DCAF8 expression in atrophic muscle and its involvement in MyHC degradation we were interested whether DCAF8 directly contributes to muscle atrophy. An established

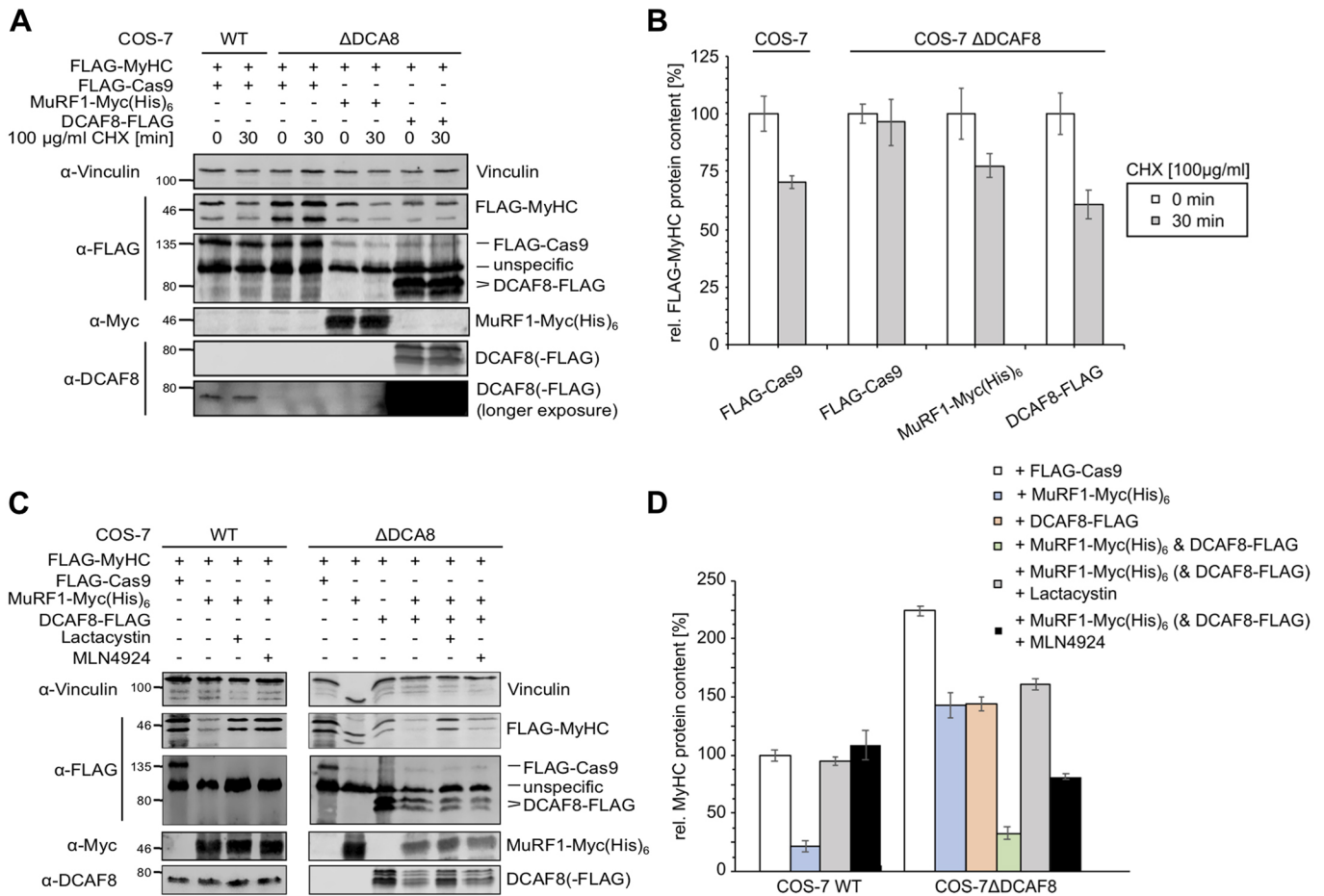


Fig. 7. Degradation of MyHC is mediated by synergistic effects of MuRF1 and DCAF8. (A) FLAG-MyHC was transiently expressed in COS-7 and COS-7 ΔDCAF8 cells and its stability was determined in a CHX decay assay. Where indicated, the COS-7 cells were co-transfected with the respective constructs. FLAG-Cas9, which is unrelated to the UPS, served as a control. (B) FLAG-MyHC signals from experiments as in A were quantified and normalized to the vinculin signals (loading control). (C) Steady-state levels of FLAG-MyHC transiently transfected into COS-7 WT and COS-7 ΔDCAF8 cells that were co-transfected with constructs for the expression of the given MuRF1 and DCAF8 constructs. Cells were treated with the proteasomal inhibitor lactacystin or the neddylation inhibitor MLN4924 where indicated. (D) FLAG-MyHC signals from experiments as in C were quantified and normalized to the vinculin signals. The resulting value for the COS-7 WT transiently transfected with FLAG-MyHC and FLAG-Cas9 was set to 100%. Results in B and D are the mean ± s.e.m. of at least three independent experiments.

method to evaluate muscle atrophy is the quantification of changes in the diameter of differentiated C2C12 myotubes after Dexamethasone (Dexa) treatment (Menconi et al., 2008; Son et al., 2015; Han et al., 2017). We downregulated DCAF8 and/or MuRF1 by siRNA in this assay to evaluate their impact in this process. Mild Dexa treatment caused a significant decrease in myotube diameter in C2C12 cells incubated with scrambled siRNA (Fig. 8C), which matches published data (Son et al., 2015; Han et al., 2017). As expected, knockdown of MuRF1 markedly impaired the Dexa-induced decrease of myotube size. Strikingly, the reduction of myotube diameter was also inhibited upon knockdown of DCAF8. In this assay, the combined downregulation of DCAF8 and MuRF1 prevented shrinkage of the myotubes to approximately the same extent as the single knockdowns (Fig. 8E). These findings support the notion that DCAF8 and MuRF1 form a functional unit to mediate muscle atrophy in cultured myotubes.

DISCUSSION

Identification of new MuRF-interacting proteins

Both the dynamic adaptation of muscle mass to cellular stimuli and the quality control in muscle cells relies on the balance of the

synthesis of sarcomeric proteins and their turnover by the ubiquitin proteasome system (UPS). Key components of this process are the MuRF1, MuRF2 and MuRF3 proteins, which have been implicated in the degradation of sarcomeric proteins like MyHC. In this work, we employed Y2H screens to identify a first set of novel putative MuRF interaction partners. This screening method is based on overexpressed bait and prey proteins in non-muscle cells. Thus, we sought to re-examine our results by SILAC-AP-MS of epitope-tagged overexpressed MuRF proteins, and identified 43 myocyte proteins that were also found in the Y2H approach. As the SILAC-AP-MS approach can also yield candidates that unspecifically bind to the overexpressed MuRF proteins, we confirmed our findings in co-IP experiments with transfected constructs in heterologous COS-7 cells and, in the case of DCAF8 and DDB1, also in co-IPs of endogenous proteins in C2C12 myocytes.

In summary, we report on the identification of cellular factors that specifically associate with MuRF1, MuRF2 and MuRF3. These newly identified binding partners may either represent substrates of the MuRF proteins or constitute co-factors that modulate their activity. MYLK2, a protein kinase that is required for the induction of muscle contraction, was among the most

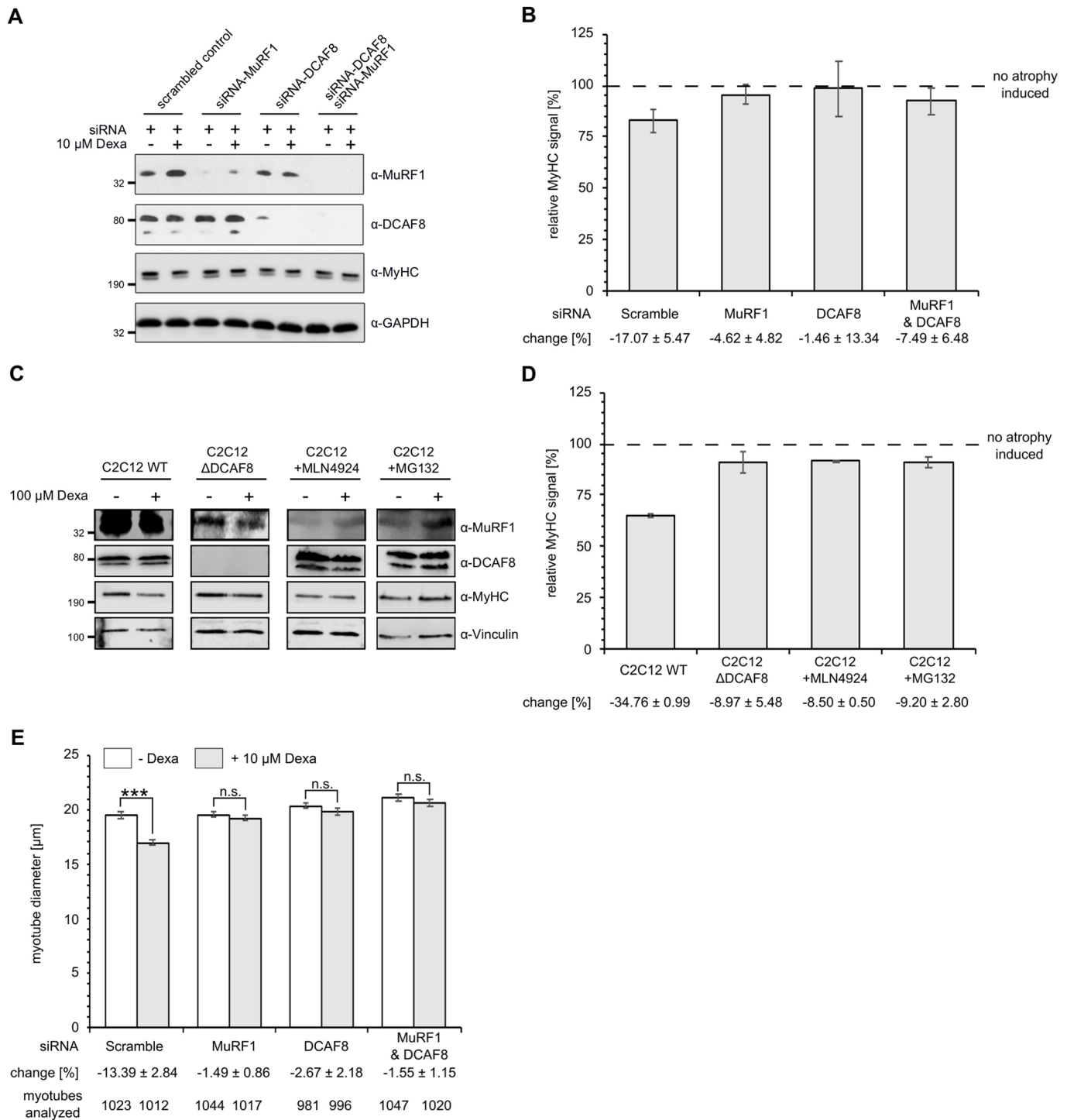


Fig. 8. DCAF8 promotes the degradation of MyHC by MuRF1. (A, B) Relative MyHC signals upon mild atrophy induction by 10 μM Dexamethasone (Dexa) for 48 h in C2C12 myotubes. MyHC signals were stable if either MuRF1 and/or DCAF8 were downregulated by siRNA. (C, D) Strong atrophy induction (100 μM Dexa, 24 h) reduces the MyHC content in C2C12 WT myotubes but not in C2C12 ΔDCAF8 myotubes. Inhibition of CRL activity by MLN4924 or treatment with the proteasomal inhibitor MG132 reduces the MyHC turnover as well, indicating that CRL-type E3 ligases and DCAF8 are crucial mediators of sarcomeric protein loss during muscle atrophy. A and C are representative blots of three independent experiments. For B and D, immunoblot signals of MyHC were quantified, normalized to the GAPDH or vinculin loading control signals and the MyHC signal of vehicle treated cells was set to 100% (highlighted by the dashed line). Then the percentage change between the samples with and without Dexa was calculated. Bar graphs represent the mean ± s.e.m. values of three independent experiments. (E) Mild atrophy induction by 10 μM Dexa reduced the diameter of C2C12 myotubes within 48 h. This effect was significantly reduced if either MuRF1 and/or DCAF8 were downregulated by siRNA. Results are the mean ± s.e.m. of the number of analyzed myotubes shown in the figure. n.s., not significant; *** $P < 0.001$ (Student's *t*-test).

prominent hits in our analysis. Remarkably, MuRF1 was previously shown to target muscle-specific creatine kinase and thereby fine-tune muscle energy metabolism (Koyama et al.,

2008). Our data now suggest that MYLK2 represents another factor for the control of muscle function that is regulated by MuRF-dependent proteolysis.

DCAF8 is involved in MyHC degradation during atrophy

In our proteome-wide screens, we identified DCAF8, a member of the DDB1 and Cul4-associated Factor (DCAF) family, as a stable interaction partner of MuRF1 and MuRF3. Our data now show a direct involvement of DCAF8 in MyHC degradation. At a first glance, the functional implications of this finding remain unclear. In COS-7 cells, DCAF8 alone is able to target ectopically expressed MyHC for proteasomal degradation. Notably, these cells do not contain endogenous muscle myosin nor do they accomplish atrophy-like processes. The co-expression of MuRF1 in such cells induces the turnover of MyHC even in absence of DCAF8. Most likely, some of the MyHC is cleared from COS-7 cells via a DCAF8-dependent quality control system that probably targets the highly abundant ectopically expressed MyHC to prevent proteotoxic stress. The addition of MuRF1 to these cells may then mobilize an additional and more specific proteolytic pathway. By contrast, MuRF1 and DCAF8 seem to co-operate in MyHC degradation in C2C12 myotubes. These cells contain endogenous DCAF8 and MuRF1 and generally constitute a far more suitable system to study muscle biogenesis. Downregulation of DCAF8 or MuRF1 or the combined loss of both factors impairs the turnover of endogenous MyHC to a similar extent. This implies that these proteins act in the same pathway for MyHC degradation in myotubes. Importantly, DCAF8 and MuRF1 levels increase in response to atrophic stimuli in C2C12 cells, and the individual or combined loss of these proteins impedes Dexamethasone-induced morphological transformations to a comparable extent. Our data therefore support a model for a collaborative activity of DCAF8 and MuRF1 in MyHC degradation during muscle atrophy.

MuRF1 and DCAF8 link CRL4 ligase complexes to muscle atrophy

DCAF proteins typically constitute substrate receptors for CRL4 ubiquitin ligase complexes. Indeed, a DCAF8-containing CRL4A complex was recently shown to ubiquitylate histone H3 in non-muscle cells, which is important for postnatal liver maturation (Li et al., 2017). Notably, CRL4A–DCAF8 complexes seem to be important factors for the development and/or homeostasis of neuronal cells. Mutations in the gene encoding DCAF8, which reduce its association with DDB1, were recently associated with the development of a HMSN2 variant. This hereditary sensory neuropathy of the extremities results in progressive muscular atrophy (Klein et al., 2014). Although, in this disease, muscular atrophy is a secondary affect, this observation already indicated an important role of DCAF8 and therefore of CRL4-type ligase complexes in muscle biology. We now confirm that DCAF8 associates, via the adaptor DDB1, with a cullin-type ligase encompassing CUL4A and RBX1. Surprisingly, this complex also interacts with the RING-finger protein MuRF1.

In most cases, CRL-type ubiquitin ligases contain a single RING-finger protein, RBX1 or RBX2, which stimulates the transfer of ubiquitin from a ubiquitin conjugating enzyme to an acceptor site within a substrate (Petroski and Deshaies, 2005; Jackson and Xiong, 2009; Sarikas et al., 2011). However, a Cul4A complex harboring two of such proteins has already been reported: COP1, a RING-finger protein that was initially thought to constitute an autonomous ubiquitin ligase, turned out to be an integral component of a CRL4A ubiquitin ligase for the degradation of c-Jun (Wertz et al., 2004). Within this complex, RBX1 is required for substrate ubiquitylation, while COP1 apparently serves different functions like defining the target range of the ubiquitin ligase (Wertz et al., 2004). Our results now suggest that topologically similar CRL4A complexes encompassing two RING finger proteins are formed in myocytes.

Functional role of the MuRF1 association with CRL4 complexes

What would be the role of the interaction of MuRF1 and a CRL4A ligase in myocytes? In analogy to COP1, the recruitment of CRL4A to MuRF1 could specify the selection of MuRF1 substrates. We noticed that MuRF1 binds to Sqstm1 isoform 1 but not to the isoform 2, which lacks 84 amino acids at its N-terminus (Fig. S6). In contrast, DCAF8 binds both Sqstm1 species. This implies that DCAF8 and MuRF1 interact with different regions in a client protein. Such divergent binding properties may expand the substrate range of MuRF1 and/or the CRL4A ligase. Indeed, MuRF1 and DCAF8 establish separate routes for the proteolysis of MyHC in the heterogeneous COS-7 cell system indicating that each of these proteins alone is capable of targeting proteins for degradation. Since MuRF1 directly binds to DDB1 and associates with the CRL4A complex even in the absence of DCAF8, this RING-finger protein may interact with several CRL4A ubiquitin ligases exposing distinct preferences for target proteins. Intriguingly, we observed that in some cellular areas the DCAF8 and MuRF1 staining did not overlap. Hence, a MuRF1–CRL4A complex in myocytes may dynamically recruit different DCAF substrate receptors to target a specific subset of sarcomeric proteins for degradation. Future mass spectrometric analysis of gene-edited myocytes will elucidate the formation of such MuRF–CRL4 complexes. Owing to the lack of appropriate antibodies we could not investigate whether MuRF1 also associates with other CRL4 components like additional DCAF proteins, Cul4B or RBX2.

Alternatively, the CRL4A complex may assist MuRF1 in the ubiquitylation of its targets. In some instances, the generation of poly-ubiquitin on substrate proteins occurs in discrete steps that each rely on the activity of distinct enzymes (Weber et al., 2016). The processing of appointed proteins during atrophy may require an initial ubiquitylating event, which then initiates the generation of the proteasomal targeting signal by a different ubiquitin ligase. MuRF1 has been reported to act as an autonomous E3-ligase (Fielitz et al., 2007a) and, to our knowledge, neither CRL4-type ligases nor DCAF8 have been previously suggested to associate with MuRF1. Thus, previous *in vitro* studies on MuRF1 substrate ubiquitylation only contained a minimal set of components, in particular the E1 and an E2 enzyme, MuRF1, ATP, ubiquitin and a substrate protein. The addition of purified CRL4A components to such reactions may reveal new insights into how the interplay of these components facilitate the degradation of sarcomeric proteins, for example, by accelerating their ubiquitylation and/or by forming distinct poly-ubiquitin signals.

However, resolving this interesting question requires the establishment of a powerful *in vitro* system with purified components to reconstitute the precise molecular mode of action of MuRF1 and CRL4A(–DCAF8) substrate ubiquitylation. Establishing this system surpasses the focus of the presented work due to the complexity of the involved machinery but will be pursued in future studies.

Role of CRL4A complexes in muscle atrophy

Aside from the now described CRL4A complex, other cullin-type ubiquitin ligases have been implicated in the regulation of muscle mass. The F-box proteins atrogin-1 and muscle ubiquitin ligase of SCF complex in atrophy-1 (MUSA1, also known as FBXO30) serve as substrate receptors of Skp1–cullin1–F-box (SCF) E3 ligase complexes (Bodine and Baehr, 2014). Similar to MuRF1 and DCAF8, the expression of these proteins is upregulated during muscle atrophy and downregulation of either factor in a model

system affects this process. Notably, CRL1 ligases encompassing atrogen-1 or MUSA1 seem to control muscle waste by targeting transcription factors for degradation. In contrast, we describe here that CRL4A complexes directly promote the turnover of the sarcomeric protein MyHC and thereby facilitate atrophy.

Our work also revealed a stable association of MuRF3 with DCAF8. While we did not investigate the nature of this interaction in more detail, this observation suggests a functional relationship between a DCAF8-containing CRL4 complex and MuRF3, similar to our observations on DCAF8, CRL4A-type ligases and MuRF1. Again, such a complex may target a different protein pool from the MuRF1–DCAF8–CRL4A axis and represent an adaptation to fine-tune the complex proteolytic events during muscle atrophy. We also observed a physical interaction of MuRF3 and the F-box protein FBXW2, indicating that the individual MuRF proteins can direct also other CRL complexes to muscle-specific functions.

Further work is required to characterize the MuRF–CRL relationship in more detail, to determine the molecular function and the regulation of their components, and to identify their target proteins. Given that the MuRF proteins directly facilitate the turnover of sarcomeric proteins, research on these ubiquitin ligases is of medical importance, because it may reveal very specific entry points for the treatment of pathogenic muscle atrophy.

MATERIALS AND METHODS

Plasmids

cDNA expression plasmids were generated using standard cloning techniques and their identity was verified by sequencing. Plasmids used in this study were: pGEM-T (Promega); pZsGreen1-C1, pZsGreen1-N1, pMCherry-C1, pmCherry-N1 (Clontech); pcDNA3.1(–), pcDNA3.1(+)-FLAG (Invitrogen), pGEX-6P-1 (GE Healthcare); and pMAL–c2x, pMAL–c4e (NEB); pQE30, pQE60 (QIAGEN). Y2H expression plasmids were generated with the Gateway technology (Invitrogen) as recommended by the manufacturer. Y2H vectors were: pDONR221 (Invitrogen), used as entry vector, and pBTM116-D9 and pACT4-DM (Goehler et al., 2004; Stelzl et al., 2005; Suter et al., 2013), as bait and prey destination vectors, respectively. Additionally, pFLAG-CMV-D11 (FLAG-tagged destination vector) was used for co-IP experiments (Invitrogen). pcDNA3-FLAG-DDB1 (Addgene #19918) and pcDNA3-HA2-DDB1 (Addgene #19909), deposited by Yue Xiong (Hu et al., 2008), were also used.

Antibodies

Anti-Myc (Sigma-Aldrich M5546; 1:1000), anti-FLAG (Sigma-Aldrich F3165; 1:400 or Cell Signaling #2368; 1500), anti-HA (Sigma-Aldrich H9658; 1:1000) and anti-Myc (Millipore 06-549; 1:500) were used for immunodetection of epitope-tagged proteins. Anti-HA (Thermo Fisher Scientific PA1-985, IP: 5 µg), anti-DCAF8 [Bethyl Laboratories, Inc. A301-556A and A301-557A; immunoblotting (IB): 1:500–1:1000, immunohistochemistry (IHC): 1:50–1:100, IP: 5 µg], anti-DDB1 (Bethyl Laboratories, Inc. A300-462A; IB: 1:500–1:1000, IP: 5 µg), anti-Cul4A (Bethyl Laboratories, Inc. A300-739A; 1:500), anti-RBX1 (Cell Signaling #11922; IB: 1:1000), anti-β-actin (Cell Signaling #4967; 1:1000), anti-MuRF1 (abcam ab57865; IB: 1:500, IHC: 1:50–1:100), anti-GAPDH (Millipore MAB374; 1:30,000), anti-USP13 (Thermo Fisher Scientific, PA5-3122; 1:1000), anti-USP35 (Novusbio, NBP1-28733; 1:1000), anti-vinculin (Sigma-Aldrich SAB4200080; 1:1000) and anti-MyHC chain (MF20) (R&D Systems, MAB4470; 1:1000) were used for immunodetection of endogenous proteins in IB or IHC experiments or for IP. A polyclonal anti-MuRF1 antibody was generated by immunizing rabbits with a C-terminal fragment (aa 185–355) of *Mus musculus* MuRF1 (–GST) purified from *E. coli* (IB: 1:500). Secondary antibodies were: horseradish peroxidase-coupled antibodies (Sigma-Aldrich A9044 and A0545; 1:10,000) and IRDye 680RD anti-mouse-IgG for immunodetection by enhanced chemiluminescence or fluorescence emission; for immunohistochemistry detection: Alexa Fluor 488 and 555 (Invitrogen A11001 and A21422; 1:500).

Cell culture

African green monkey fibroblast (COS-7, CRL-1651), mouse skeletal muscle myoblast (C2C12, CRL-1772), and rat cardiac muscle myoblast (H9c2, CRL-1446) cells were received from the American Type Culture Collection (ATCC), cultured and maintained as recommended by the ATCC. C2C12 myoblast cells were differentiated into myotubes by reducing the FBS (PAA, A15-151) concentration of the culture medium from 10% to 2% for at least 5 days. COS-7 and C2C12 cells were transfected with plasmid DNA using Lipofectamine 300 and P3000 reagent or Lipofectamine and PLUS reagent (Invitrogen), respectively, as recommended by the manufacturer. H9c2 cells were transduced with adenovirus (AdV) to express Myc(His)₆ fusions of MuRF1, 2 or 3 for SILAC-AP-MS analysis. A promoterless adenovirus (AdV-PL) was used as control. All adenovirus were generated by SIRION BIOTECH (Martinsried, Germany). H9c2 cells were transduced with a multiplicity of infection (MOI) of 200 and incubated for at least 24 h. Subsequent protein synthesis was allowed in all experiments for at least 48 h. To reduce the protein amount of DCAF8 (catalog number L-054718-01-0005) and MuRF1 (catalog number L-067480-01-0005), C2C12 cells were transfected with the respective commercially available ON-TARGETplus siRNA SMARTpool (Dharmacon Inc) or with non-targeting scrambled (catalogue number: D-001810-10-05) siRNA. 25 nM siRNAs were transfected using DharmaFECT3 according to the manufacturer's instructions for 72–96 h (medium renewal after 24 h). DCAF8 (catalog number: L-013062-01-0005) was knocked down in COS-7 cells with DharmaFECT2.

SILAC-AP-MS screening

H9c2 cells were grown in medium supplemented with either light (lysine-0, arginine-0) or heavy (lysine-8, arginine-10) SILAC amino acids (aa) for 24 h. The SILAC-labeled H9c2 cells were transduced with Adv containing either a control plasmid (labeled with light aa) or the MuRF [MuRF1–Myc(His)₆, MuRF2–Myc(His)₆ or MuRF3–Myc(His)₆] expression plasmid (heavy aa). After transduction, surplus Adv was removed by washing and protein synthesis was allowed for 48 h. APs with TALON Metal Affinity Resin was then performed as described above. In each experiment, the SILAC labeling efficiency was ≥94%.

Mass spectrometric analysis

Proteins isolated by the APs were dissolved in 6 M urea, 2 M thiourea, 20 mM Hepes pH 8.0. Disulfide bonds were first reduced with dithiothreitol (DTT) and then cysteine groups were alkylated with 2-chloroacetamide (CAA). The proteins were proteolyzed with Lys-C and trypsin in a two-step procedure (Kanashova et al., 2015). Peptides were extracted, desalted and stored on reversed-phase (C18) StageTips (Ishihama et al., 2006). After elution, the peptides were lyophilized and resolved in 3% trifluoroacetic acid (TFA), 5% acetonitrile in preparation for LC-MS analysis. Peptides were separated on a 15 cm in-house made reverse-phase column, 75 µM ID, 3 µM C18 (Dr Maisch) by a gradient from 4% to 42% B in 135 min, with a flow-rate of 300 nl/min, and detected on a LTQ-Orbitrap XL. MS acquisition was performed at a resolution of 60,000 in the scan range from 300 to 170 *m/z*. The MS/MS spectra were collected in the LTQ part of the instrument with the dynamic exclusion set to 30 s. The data were processed using the MaxQuant software package (Cox and Mann, 2008) with the rat IPI-database v3.87, Cysteine carbamylation set as a fixed and methionine oxidation as a variable modification. Peptides with heavy:light (H:L) ratios higher than 1.5 were considered to be enriched with the corresponding MuRF protein.

Yeast two-hybrid screening

High-throughput cytosolic yeast two-hybrid (Y2H) screenings were performed to identify new MuRF-interacting proteins. Therefore, we performed an automated Y2H pipeline, as described previously (Goehler et al., 2004; Stelzl et al., 2005). In short, MuRF full-length and N- or C-terminal truncated cDNA domain constructs (Fig. S1) were cloned into suitable Y2H LexA DNA-binding domain fusion bait vectors and transformed into the MATa strain carrying *HIS3*, *URA3*, and *LacZ* as reporter genes. Bait constructs were tested for the ability to auto-activate the reporter genes (Table S1). Non-auto-activating MuRF-bait cDNA constructs were individually screened four times against a library of

23,000 individual prey clones (covering ~75% of the human protein coding genome) bearing Gal4 transcription activation domain hybrids in the L40cccMAT α strain. Bait–prey mating took place by mixing 384-microtiter plates and spotting the mixture on yeast complete medium solid agar plates. After growth, the colonies were transferred to SD selective medium lacking leucine and tryptophan to select diploid cells. These cells were then spotted on SD agar plates lacking leucine, tryptophan, uracil and histidine (SD4 plates) and covered with a nylon membrane. After 4 days of growth a β -galactosidase activity assay was performed with the nylon membranes. We then calculated a composite Y2H score based on the growth on the SD4 plates (Gal4) and the results from the β -galactosidase measurements (*LacZ*). As the activation of the *LacZ* reporter is more difficult to detect and represents a more stringent output, we weighted it two-fold. Since the screening was repeated four times, the maximum score of 12 was set to 1. Proteins with a score of 0.3 and higher were considered positive screening hits.

$$Y2Hscore = \frac{GAL4(n) + LacZ(n) * 2}{12} \quad (1)$$

Protein–protein interaction database

The protein interactions from this publication have been submitted to the IMEx (www.imexconsortium.org) consortium through IntAct (Orchard et al., 2014) and assigned the identifier IM-25805.

Protein–protein interaction network

The protein–protein interaction (PPI) network shown in Fig. 1B was generated with Cytoscape 2.8.2 (Shannon et al., 2003) and shows all the PPI that were validated in co-IP experiments.

Immunofluorescence microscopy

For immunofluorescence microscopy, cells were plated on coverslips coated with gelatin (Sigma, G1393), transfected with the indicated constructs and, 24 h later, fixed for 20 min with 4% (v/v) paraformaldehyde in PBS. Coverslips were then washed with PBS and treated with PBS containing 0.2% Triton X-100 for 20 min at room temperature. After another wash with PBS, the samples were incubated with either 5% (v/v) goat serum or bovine serum albumin. The fixed cells were then incubated overnight at 4°C with the primary antibody, washed with PBS, and incubated for 1 h with the secondary antibody at room temperature. Afterwards, cells were washed three times with PBS and mounted with ProLong[®] Gold antifade reagent containing DAPI (Thermo Fisher Scientific, 36931). The actin cytoskeleton was visualized with phalloidin conjugated to FITC (green) or –TRITC (red); fixed and permeabilized cells were incubated with 1 μ M FITC or TRITC (0.5 mg/ml) in 100 μ l PBS for 40 min at room temperature, subsequently washed with PBS and mounted. All images were acquired with an inverted fluorescence microscope (Axio Observer Z1, Zeiss) using a cooled CCD camera (AxioCam MRm) and AxioVision (rel. 4.7.2.0) software.

Generation of stable knockout cells using CRISPR/Cas9

Stable C2C12 DCAF8-knockout cells were generated using the CRISPR/Cas9 technique (Ran et al., 2013). In brief, guide oligonucleotides targeting exon 2 of murine DCAF8 were designed using the CRISPOR web tool (www.crispor.tefor.net/crispor.py). The oligonucleotides were annealed and cloned according to the Zhang lab protocol (accessed via www.addgene.org/crispr/zhang/) into a modified pX330 vector coding also for a mCherry-tagged Cas9 (a kind gift of Dr Ralf Kühn, MDC Berlin). C2C12 cells were then transfected as described above. At 36 h post transfection single mCherry-positive cells were sorted by the MDC-FACS Core Facility. Individual clones were expanded and the DCAF8 knockout was verified by immunoblotting and sequencing of the genomic locus. To this end, genomic DNA was extracted (QuickExtract[™] DNA Extraction Solution 1.0, Epicentre), the locus of DCAF8 exon 2 was PCR-amplified and the amplicon sequenced. Guide sequence and oligonucleotides used to generate stable DCAF8 knockout C2C12 cells were: guide sequence (including PAM), 5'-GCACCGTGGACAGCGCAAACGGG-3'; oligonucleotide 1 (including overhang for BbsI cloning into pX330), 5'-CACCGCACCGTGGACAGCGCAAAC-3'; oligonucleotide 2 (including overhang for BbsI

cloning into pX330), 5'-AAACGTTTGCCTGTCCACGGTGC-3'; validation primer forward direction, 5'-GCAAACCTGAAACCTGAGGC-3'; validation primer reverse direction, 5'-GCTGTAGGCTCCTGGATGTG-3'. Validation primers were used for amplification and sequencing of DCAF8 exon 2.

Affinity purifications and immunopurifications

Affinity purifications (AP) and immunopurifications of Myc(His)₆- or FLAG-tagged proteins from eukaryotic cells was performed in a 50 mM phosphate buffer pH 7.4 containing 150 mM NaCl. This lysis buffer was supplemented with cOmplete protease inhibitor cocktail (Roche) and 0.5–1% (v/v) Triton X-100. The cells were lysed on a rotating wheel for 30 min at 4°C and lysate was cleared by centrifugation (16,000 g, 4°C, 10 min). His-APs were performed using TALON Metal Affinity Resin (Clontech) in presence of 10 mM imidazole in the lysis buffer over night at 4°C and after washing of the beads with lysis buffer bound proteins were eluted with 200 mM imidazole in lysis buffer. For FLAG immunopurifications, the lysate was incubated with anti-FLAG M2 Affinity Gel (Sigma-Aldrich, A2220) at 4°C for 1 to 4 h and after washing of the beads the bound material was eluted by boiling (95°C, 10 min) in protein sample buffer. Endogenous DCAF8 and DDB1 were purified from C2C12 cell lysates with 5 μ g of anti-DCAF8 or anti-DDB1 antibodies and protein G–Sephacryl (GE healthcare, 50 μ l slurry) overnight at 4°C and after washing eluted from the beads in protein sample buffer. Samples were analyzed by SDS-PAGE and immunoblotting. The signals were visualized with specific antibodies and horseradish peroxidase-coupled antibodies using Western Lightning Plus-ECL (PerkinElmer) in a LI-COR Odyssey FC according to the manufacturer's instructions.

Generation of an anti-MuRF1 antibody

A region encoding aa 185–355 of mouse MuRF1 (Fig. S4) was cloned into pGEX-6P-1 and the resulting construct transformed into *E. coli* BL21 cells. The expression of a MuRF1–GST fusion construct was induced by the addition of 0.5 mM IPTG for 4 h. The *E. coli* cells were lysed in a French press and the lysate cleared by centrifugation at 17,200 g at 4°C for 30 min. GST purifications were performed using glutathione–Sephacryl 4 fast flow (GE Healthcare) and eluted by cleaving the GST tag with GST-tag PreScission protease according to the manufacturer's instructions. Rabbits were then immunized three times by injecting 200 μ g of purified MuRF1 protein. The specificity of the antiserum was tested in immunoblots using lysates of muscle cells derived from WT, MuRF1 knockout or MuRF1/MuRF3 double knockout mice (Fig. S4B).

Cycloheximide decay assays and steady state analysis

COS-7 cells were transfected with the given constructs and after 24–48 h the translation of polypeptides was inhibited by adding 100 μ g/ml cycloheximide (CHX). Cells were harvested at the given time points after CHX addition, lysed as mentioned above, boiled with protein sample buffer, and analyzed by SDS-PAGE and immunoblotting. Quantitative analysis of the immunoblots was performed with fluorescently labeled secondary antibodies and LI-COR Odyssey FC using the Image Studio[™] Lite (LI-COR Biosciences) or FIJI software (Schindelin et al., 2012). For steady state analysis, cells were transfected and harvested after 48 h of transient expression of the respective constructs. Where indicated, 1 μ M of MLN 4924 (Boston Biochem) or 5 μ M lactacystin were added 4 h prior to cell harvest in order to inhibit neddylation, and thereby activation of CRL-ligases, or in order to inhibit the proteasome, respectively. The FLAG-tagged motor region of myosin heavy chain 7 (FLAG–MyHC) was used as substrate (Fielitz et al., 2007a). Transiently expressed FLAG-tagged Cas9, which is not related to the UPS, served as control.

Atrophy assays

C2C12 myotubes were transfected with siRNA to inhibit expression of the given genes and atrophy was induced by adding 10 μ M Dexa for 48 h (mild atrophy induction). The progress of atrophy was determined by measuring the diameter of myotubes. Cell images were captured at 20 \times total magnification using an inverted fluorescence microscope (Axio Observer Z1, Zeiss) and a cooled CCD camera (AxioCam MRm). At least ten random

pictures per experiment were taken and, in each sample, the diameter of 10–20 myotubes was quantified using the Zeiss AxioVision software. Each myotube was measured at its ends and in the middle in three double-blind experiments. Mean±s.e.m. values were calculated and Dexa-treated cells were compared with untreated myotubes. After imaging cells were harvested, boiled in sample buffer, and analyzed by SDS-PAGE and immunoblotting. For strong atrophy induction, 100 μM Dexa was added to C2C12 myotubes for 24 h. Where indicated, 1 μM MLN4924 (BostonBiochem) or 12.5 μM MG132 (Sigma) in 0.05% DMSO (v/v, final concentration) was added to the medium to inhibit neddylation of CRL complexes and the proteasome, respectively.

Animal experiments

Denervation experiments were performed as published (Schmidt et al., 2014). Briefly, skeletal muscle atrophy was induced in adult male C57BL/6N mice (6–8 weeks of age) by dissection of the left sciatic nerve. Mice were anesthetized with isoflurane, placed on a heating pad to assure a constant body temperature of 37°C, as measured by a rectal probe. The sciatic nerve of the left leg was cut and a 3 mm piece was excised (defined as the denervated sample). The right leg remained innervated and was used as control (defined as the innervated control). Mice were killed at baseline after 7, 14 and 21 days of surgery ($n=6$). *Gastrocnemius plantaris* and *tibialis anterior* muscles were obtained, snap frozen in liquid nitrogen and stored at –80°C until further analysis. The skeletal muscle mass as well as the length of the tibia served as a reference.

Study approval

All animal procedures, denervation and food deprivation, were performed in accordance with the guidelines of the Max-Delbrück Center for Molecular Medicine and the Charité-Universitätsmedizin Berlin and were approved by the Landesamt für Gesundheit und Soziales (LaGeSo, Berlin, Germany) for the use of laboratory animals (permit number G 0129/12). These rules follow the ‘Principles of Laboratory Animal Care’ (NIH publication No. 86-23, revised 1985) and the current version of German Law on the Protection of Animals.

Statistics

Data are presented as mean±s.e.m. Differences between indicated myotube groups were analyzed by two-sided unpaired Student’s *t*-tests. Statistical analysis was performed using Microsoft Excel®. $P>0.05$ was taken as not significant (n.s.); $*P\leq 0.05$, $**P\leq 0.01$, $***P\leq 0.001$.

Acknowledgements

We thank all authors for comments on the manuscript. We thank Ernst Jarosch and Friedrich C. Luft for editing the manuscript. Ernst Jarosch is acknowledged for his help in the anti-MuRF1 antibody production. We thank Raymond J. Deshaies for discussion of CRL4 complex-related results. We thank Ralf Kühn for the modified pX330, Ines Lahmann (Carmen Birchmeier lab) and Christin Suenkel (Nikolaus Rajewsky lab) for technical advice on CRISPR/Cas9 experiments, and the MDC FACS core facility for cell sorting. We thank Corinna Volkwein, Mandy Mustroph and Angelika Wittstruck for excellent technical assistance.

Competing interests

The authors declare no competing or financial interests.

Author contributions

Conceptualization: J.F., T.S.; Methodology: E.E.W., G.D., J.F.; Investigation: M.N., B.S., P.P., R.M., F.S., M.K., X.Z.; Writing - original draft: B.S.; Writing - review & editing: M.N., J.F., T.S.; Visualization: M.N.; Supervision: B.S., T.S.; Project administration: T.S.; Funding acquisition: E.E.W., J.F., T.S.

Funding

The Deutsche Forschungsgemeinschaft (FI 965/4-1 and SO 271/6-1), the Max-Delbrück-Center for Molecular Medicine, and the Experimental and Clinical Research Center (ECRC) supported this work. This study also received funding from the GO-Bio Initiative of the German Federal Ministry for Education and Research (Bundesministerium für Bildung und Forschung; BMBF), grant no. 0313881, the ERA-NET NEURON initiative, funded by the BMBF, grant no. 01W1301, the Berlin Institute of Health Collaborative Research grant no. 1.1.2.a.3 funded by the BMBF, and the Helmholtz Validation Fund funded by the Helmholtz Association, Germany, grant no. HVF-0013 (to E.E.W.).

Data availability

The protein interactions from this publication have been submitted to the IMEx (www.imexconsortium.org) consortium through IntAct (Orchard et al., 2014) and assigned the identifier IM-25805.

Supplementary information

Supplementary information available online at <http://jcs.biologists.org/lookup/doi/10.1242/jcs.233395.supplemental>

References

- Angers, S., Li, T., Yi, X., Maccoss, M. J., Moon, R. T. and Zheng, N. (2006). Molecular architecture and assembly of the DDB1–CUL4A ubiquitin ligase machinery. *Nature* **443**, 590–593. doi:10.1038/nature05175
- Blondelle, J., Shapiro, P., Domenighetti, A. A. and Lange, S. (2017). Cullin E3 ligase activity is required for myoblast differentiation. *J. Mol. Biol.* **429**, 1045–1066. doi:10.1016/j.jmb.2017.02.012
- Bodine, S. C. and Baehr, L. M. (2014). Skeletal muscle atrophy and the E3 ubiquitin ligases MuRF1 and MAFbx/atrogen-1. *Am. J. Physiol. Endocrinol. Metab.* **307**, E469–E484. doi:10.1152/ajpendo.00204.2014
- Bodine, S. C., Latres, E., Baumhueter, S., Lai, V. K., Nunez, L., Clarke, B. A., Poueymirou, W. T., Panaro, F. J., Na, E., Dharmarajan, K. et al. (2001). Identification of ubiquitin ligases required for skeletal muscle atrophy. *Science* **294**, 1704–1708. doi:10.1126/science.1065874
- Buetow, L. and Huang, D. T. (2016). Structural insights into the catalysis and regulation of E3 ubiquitin ligases. *Nat. Rev. Mol. Cell Biol.* **17**, 626–642. doi:10.1038/nrm.2016.91
- Castillero, E., Alamdari, N., Lecker, S. H. and Hasselgren, P.-O. (2013). Suppression of atrogen-1 and MuRF1 prevents dexamethasone-induced atrophy of cultured myotubes. *Metabolism* **62**, 1495–1502. doi:10.1016/j.metabol.2013.05.018
- Centner, T., Yano, J., Kimura, E., Mcelhinny, A. S., Pelin, K., Witt, C. C., Bang, M.-L., Trombitas, K., Granzier, H., Gregorio, C. C. et al. (2001). Identification of muscle specific ring finger proteins as potential regulators of the titin kinase domain. *J. Mol. Biol.* **306**, 717–726. doi:10.1006/jmbi.2001.4448
- Clarke, B. A., Drujan, D., Willis, M. S., Murphy, L. O., Corpina, R. A., Burova, E., Rakhilin, S. V., Stitt, T. N., Patterson, C., Latres, E. et al. (2007). The E3 ligase MuRF1 degrades myosin heavy chain protein in dexamethasone-treated skeletal muscle. *Cell Metab.* **6**, 376–385. doi:10.1016/j.cmet.2007.09.009
- Cohen, S., Brault, J. J., Gygi, S. P., Glass, D. J., Valenzuela, D. M., Gartner, C., Latres, E. and Goldberg, A. L. (2009). During muscle atrophy, thick, but not thin, filament components are degraded by MuRF1-dependent ubiquitylation. *J. Cell Biol.* **185**, 1083–1095. doi:10.1083/jcb.200901052
- Cox, J. and Mann, M. (2008). MaxQuant enables high peptide identification rates, individualized p.p.b.-range mass accuracies and proteome-wide protein quantification. *Nat. Biotechnol.* **26**, 1367–1372. doi:10.1038/nbt.1511
- Fields, S. and Song, O. (1989). A novel genetic system to detect protein–protein interactions. *Nature* **340**, 245–246. doi:10.1038/340245a0
- Fielitz, J., Van Rooij, E., Spencer, J. A., Shelton, J. M., Latif, S., Van Der Nagel, R., Bezprozvannaya, S., De Windt, L., Richardson, J. A., Bassel-Duby, R. et al. (2007a). Loss of muscle-specific RING-finger 3 predisposes the heart to cardiac rupture after myocardial infarction. *Proc. Natl Acad. Sci. USA* **104**, 4377–4382. doi:10.1073/pnas.0611726104
- Fielitz, J., Kim, M.-S., Shelton, J. M., Latif, S., Spencer, J. A., Glass, D. J., Richardson, J. A., Bassel-Duby, R. and Olson, E. N. (2007b). Myosin accumulation and striated muscle myopathy result from the loss of muscle RING finger 1 and 3. *J. Clin. Invest.* **117**, 2486–2495. doi:10.1172/JCI32827
- Fioletta, V. C., White, L. J., Larsen, A. E., Léger, B. and Russell, A. P. (2011). The role and regulation of MAFbx/atrogen-1 and MuRF1 in skeletal muscle atrophy. *Pflügers Archiv Eur. J. Physiol.* **461**, 325–335. doi:10.1007/s00424-010-0919-9
- Goehler, H., Lalowski, M., Stelzl, U., Waelter, S., Stroedicke, M., Worm, U., Droege, A., Lindenberg, K. S., Knoblich, M., Haenig, C. et al. (2004). A protein interaction network links GIT1, an enhancer of huntingtin aggregation, to Huntington’s disease. *Mol. Cell* **15**, 853–865. doi:10.1016/j.molcel.2004.09.016
- Gotthardt, M., Hammer, R. E., Hübner, N., Monti, J., Witt, C. C., McNabb, M., Richardson, J. A., Granzier, H., Labeit, S. and Herz, J. (2003). Conditional expression of mutant M-line titins results in cardiomyopathy with altered sarcomere structure. *J. Biol. Chem.* **278**, 6059–6065. doi:10.1074/jbc.M211723200
- Han, D.-S., Yang, W.-S. and Kao, T.-W. (2017). Dexamethasone treatment at the myoblast stage enhanced C2C12 myocyte differentiation. *Int. J. Med. Sci.* **14**, 434–443. doi:10.7150/ijms.18427
- Hasselgren, P.-O. (1999). Glucocorticoids and muscle catabolism. *Curr. Opin. Clin. Nutr. Metab. Care* **2**, 201–205. doi:10.1097/00075197-199905000-00002
- Hershko, A. and Ciechanover, A. (1998). The Ubiquitin System. *Annu. Rev. Biochem.* **67**, 425–479. doi:10.1146/annurev.biochem.67.1.425
- Hirner, S., Krohne, C., Schuster, A., Hoffmann, S., Witt, S., Erber, R., Sticht, C., Gasch, A., Labeit, S. and Labeit, D. (2008). MuRF1-dependent regulation of systemic carbohydrate metabolism as revealed from transgenic mouse studies. *J. Mol. Biol.* **379**, 666–677. doi:10.1016/j.jmb.2008.03.049
- Hu, J., Zacharek, S., He, Y. J., Lee, H., Shumway, S., Duronio, R. J. and Xiong, Y. (2008). WD40 protein FBW5 promotes ubiquitination of tumor suppressor TSC2

- by DDB1-CUL4-ROC1 ligase. *Genes Dev.* **22**, 866-871. doi:10.1101/gad.1624008
- Ishihama, Y., Rappsilber, J. and Mann, M. (2006). Modular stop and go extraction tips with stacked disks for parallel and multidimensional peptide fractionation in proteomics. *J. Proteome Res.* **5**, 988-994. doi:10.1021/pr050385q
- Jackson, S. and Xiong, Y. (2009). CRL4s: the CUL4-RING E3 ubiquitin ligases. *Trends Biochem. Sci.* **34**, 562-570. doi:10.1016/j.tibs.2009.07.002
- Jin, J., Arias, E. E., Chen, J., Harper, J. W. and Walter, J. C. (2006). A family of diverse Cul4-Ddb1-interacting proteins includes Cdt2, which is required for S phase destruction of the replication factor Cdt1. *Mol. Cell* **23**, 709-721. doi:10.1016/j.molcel.2006.08.010
- Kanashova, T., Popp, O., Orasche, J., Karg, E., Harndorf, H., Stengel, B., Sklorz, M., Streibel, T., Zimmermann, R. and Dittmar, G. (2015). Differential proteomic analysis of mouse macrophages exposed to adsorbate-loaded heavy fuel oil derived combustion particles using an automated sample-preparation workflow. *Anal. Bioanal. Chem.* **407**, 5965-5976. doi:10.1007/s00216-015-8595-4
- Kedar, V., McDonough, H., Arya, R., Li, H.-H., Rockman, H. A. and Patterson, C. (2004). Muscle-specific RING finger 1 is a bona fide ubiquitin ligase that degrades cardiac troponin I. *Proc. Natl. Acad. Sci. USA* **101**, 18135-18140. doi:10.1073/pnas.0404341102
- Khan, M. M., Strack, S., Wild, F., Hanashima, A., Gasch, A., Brohm, K., Reischl, M., Carnio, S., Labeit, D., Sandri, M. et al. (2014). Role of autophagy, SQSTM1, SH3GLB1, and TRIM63 in the turnover of nicotinic acetylcholine receptors. *Autophagy* **10**, 123-136. doi:10.4161/autophagy.26841
- Klein, C. J., Wu, Y., Vogel, P., Goebel, H. H., Bonnemann, C., Zukosky, K., Botuyan, M.-V., Duan, X., Middha, S., Atkinson, E. J. et al. (2014). Ubiquitin ligase defect by DCAF8 mutation causes HMSN2 with giant axons. *Neurology* **82**, 873-878. doi:10.1212/WNL.0000000000000206
- Koyama, S., Hata, S., Witt, C. C., Ono, Y., Lerche, S., Ojima, K., Chiba, T., Doi, N., Kitamura, F., Tanaka, K. et al. (2008). Muscle RING-Finger Protein-1 (MuRF1) as a connector of muscle energy metabolism and protein synthesis. *J. Mol. Biol.* **376**, 1224-1236. doi:10.1016/j.jmb.2007.11.049
- Lange, S. (2005). The kinase domain of titin controls muscle gene expression and protein turnover. *Science* **308**, 1599-1603. doi:10.1126/science.1110463
- Lee, Y. J., Chou, T.-F., Pittman, S. K., Keith, A. L., Razani, B. and Weihl, C. C. (2017). Keap1/Cullin3 modulates p62/SQSTM1 activity via UBA domain ubiquitination. *Cell Rep.* **19**, 188-202. doi:10.1016/j.celrep.2017.03.030
- Li, G., Ji, T., Chen, J., Fu, Y., Hou, L., Feng, Y., Zhang, T., Song, T., Zhao, J., Endo, Y. et al. (2017). CRL4 DCAF8 ubiquitin ligase targets histone H3K79 and promotes H3K9 methylation in the liver. *Cell Rep.* **18**, 1499-1511. doi:10.1016/j.celrep.2017.01.039
- Loch, C. M. and Strickler, J. E. (2012). A microarray of ubiquitylated proteins for profiling deubiquitylase activity reveals the critical roles of both chain and substrate. *Biochim. Biophys. Acta Mol. Cell Res.* **1823**, 2069-2078. doi:10.1016/j.bbamcr.2012.05.006
- Massaccesi, L., Goi, G., Tringali, C., Barassi, A., Venerando, B. and Papini, N. (2016). Dexamethasone-induced skeletal muscle atrophy increases O-GlcNAcylation in C2C12 cells. *J. Cell. Biochem.* **117**, 1833-1842. doi:10.1002/jcb.25483
- Mcelhinny, A. S., Kakinuma, K., Sorimachi, H., Labeit, S. and Gregorio, C. C. (2002). Muscle-specific RING finger-1 interacts with titin to regulate sarcomeric M-line and thick filament structure and may have nuclear functions via its interaction with glucocorticoid modulatory element binding protein-1. *J. Cell Biol.* **157**, 125-136. doi:10.1083/jcb.200108089
- Menconi, M., Gonnella, P., Petkova, V., Lecker, S. and Hasselgren, P.-O. (2008). Dexamethasone and corticosterone induce similar, but not identical, muscle wasting responses in cultured L6 and C2C12 myotubes. *J. Cell. Biochem.* **105**, 353-364. doi:10.1002/jcb.21833
- Orchard, S., Ammari, M., Aranda, B., Breuza, L., Briganti, L., Broackes-Carter, F., Campbell, N. H., Chavali, G., Chen, C., Del-Toro, N. et al. (2014). The MintAct project—IntAct as a common curation platform for 11 molecular interaction databases. *Nucleic Acids Res.* **42**, D358-D363. doi:10.1093/nar/gkt1115
- Perera, S., Mankoo, B. and Gautel, M. (2012). Developmental regulation of MURF E3 ubiquitin ligases in skeletal muscle. *J. Muscle Res. Cell Motil.* **33**, 107-122. doi:10.1007/s10974-012-9288-7
- Petroski, M. D. and Deshaies, R. J. (2005). Function and regulation of cullin-RING ubiquitin ligases. *Nat. Rev. Mol. Cell Biol.* **6**, 9-20. doi:10.1038/nrm1547
- Ran, F. A., Hsu, P. D., Wright, J., Agarwala, V., Scott, D. A. and Zhang, F. (2013). Genome engineering using the CRISPR-Cas9 system. *Nat. Protoc.* **8**, 2281-2308. doi:10.1038/nprot.2013.143
- Sarikas, A., Hartmann, T. and Pan, Z.-Q. (2011). The cullin protein family. *Genome Biol.* **12**, 220. doi:10.1186/gb-2011-12-4-220
- Schindelin, J., Arganda-Carreras, I., Frise, E., Kaynig, V., Longair, M., Pietzsch, T., Preibisch, S., Rueden, C., Saalfeld, S., Schmid, B. et al. (2012). Fiji: an open-source platform for biological-image analysis. *Nat. Methods* **9**, 676-682. doi:10.1038/nmeth.2019
- Schmidt, F., Kny, M., Zhu, X., Wollersheim, T., Persicke, K., Langhans, C., Lodka, D., Kleber, C., Weber-Carstens, S. and Fielitz, J. (2014). The E3 ubiquitin ligase TRIM62 and inflammation-induced skeletal muscle atrophy. *Crit. Care* **18**, 545. doi:10.1186/s13054-014-0545-6
- Shannon, P., Markiel, A., Ozier, O., Baliga, N. S., Wang, J. T., Ramage, D., Amin, N., Schwikowski, B. and Ideker, T. (2003). Cytoscape: A software Environment for integrated models of biomolecular interaction networks. *Genome Res.* **13**, 2498-2504. doi:10.1101/gr.1239303
- Son, Y. H., Lee, S.-J., Lee, K.-B., Lee, J.-H., Jeong, E. M., Chung, S. G., Park, S.-C. and Kim, I.-G. (2015). Dexamethasone downregulates caveolin-1 causing muscle atrophy via inhibited insulin signaling. *J. Endocrinol.* **225**, 27-37. doi:10.1530/JOE-14-0490
- Spencer, J. A., Eliazar, S., Ilaria, R. L., Richardson, J. A. and Olson, E. N. (2000). Regulation of microtubule dynamics and myogenic differentiation by MURF, a striated muscle RING-finger protein. *J. Cell Biol.* **150**, 771-784. doi:10.1083/jcb.150.4.771
- Stelzl, U., Worm, U., Lalowski, M., Haenig, C., Brembeck, F. H., Goehler, H., Stroedicke, M., Zenkner, M., Schoenherr, A., Koeppen, S. et al. (2005). A human protein-protein interaction network: a resource for annotating the proteome. *Cell* **122**, 957-968. doi:10.1016/j.cell.2005.08.029
- Suter, B., Fontaine, J.-F., Yildirimman, R., Raskó, T., Schaefer, M. H., Rasche, A., Porras, P., Vázquez-Álvarez, B. M., Russ, J., Rau, K. et al. (2013). Development and application of a DNA microarray-based yeast two-hybrid system. *Nucleic Acids Res.* **41**, 1496-1507. doi:10.1093/nar/gks1329
- Troncoso, R., Paredes, F., Parra, V., Gatica, D., Vázquez-Trincado, C., Quiroga, C., Bravo-Sagua, R., López-Crisosto, C., Rodríguez, A. E., Oyarzún, A. P. et al. (2014). Dexamethasone-induced autophagy mediates muscle atrophy through mitochondrial clearance. *Cell Cycle* **13**, 2281-2295. doi:10.4161/cc.29272
- Weber, A., Cohen, I., Popp, O., Dittmar, G., Reiss, Y., Sommer, T., Ravid, T. and Jarosch, E. (2016). Sequential poly-ubiquitylation by specialized conjugating enzymes expands the versatility of a quality control ubiquitin ligase. *Mol. Cell* **63**, 827-839. doi:10.1016/j.molcel.2016.07.020
- Wertz, I. E., O'Rourke, K. M., Zhang, Z., Dornan, D., Arnott, D., Deshaies, R. J. and Dixit, V. M. (2004). Human de-etiololed-1 regulates c-Jun by assembling a CUL4A ubiquitin ligase. *Science* **303**, 1371-1374. doi:10.1126/science.1093549
- Witt, S. H., Granzier, H., Witt, C. C. and Labeit, S. (2005). MURF-1 and MURF-2 target a specific subset of myofibrillar proteins redundantly: towards understanding MURF-dependent muscle ubiquitination. *J. Mol. Biol.* **350**, 713-722. doi:10.1016/j.jmb.2005.05.021
- Woodsmith, J., Jenn, R. C. and Sanderson, C. M. (2012). Systematic analysis of dimeric E3-RING interactions reveals increased combinatorial complexity in human ubiquitination networks. *Mol. Cell. Proteomics* **11**, M111.016162. doi:10.1074/mcp.M111.016162

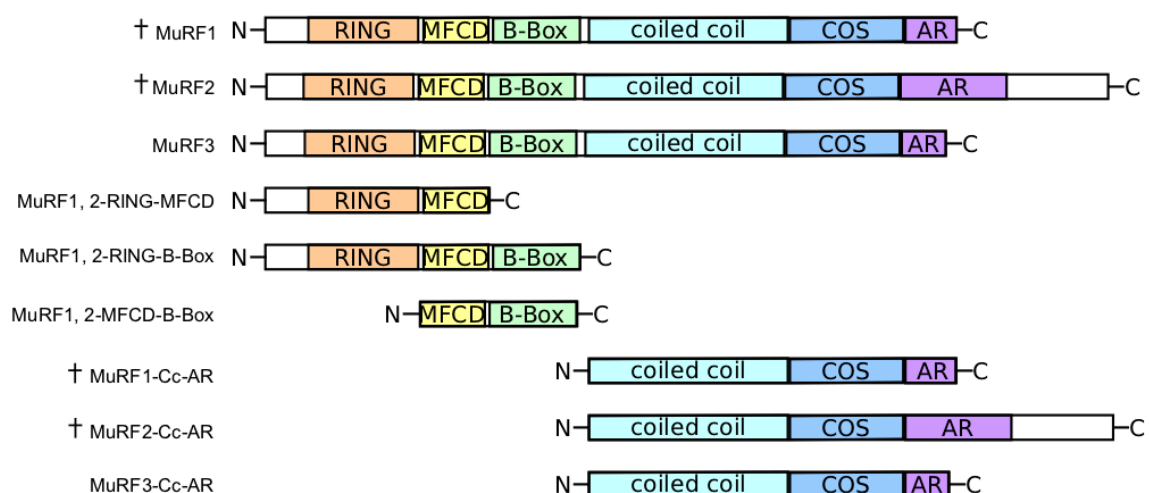


Fig. S1: HT-Y2H-Screens.

Schematic representation of MuRF full-length and N- or C-terminal truncated cDNA domain constructs used as baits in Y2H screenings. MFCD: MuRF-family-conserved domain, AR: Acidic rich region. Constructs marked with a cross auto-activated the Y2H reporter genes and were therefore not used in the screening procedure.

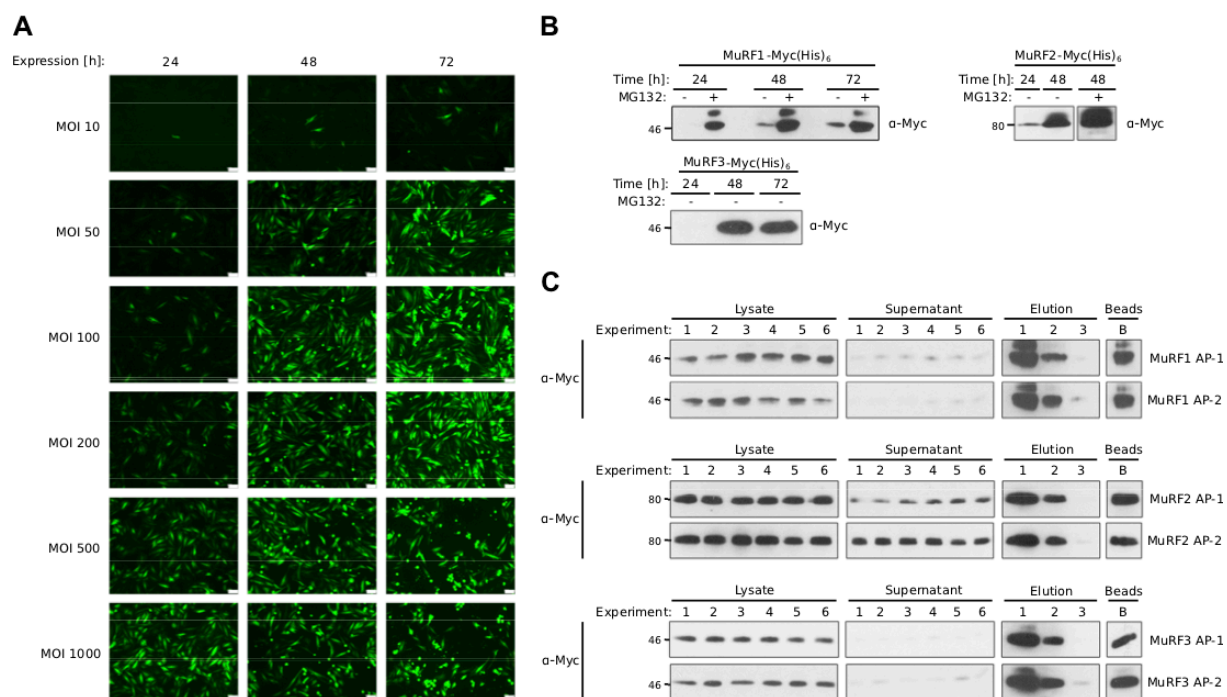


Fig. S2: SILAC-AP-MS experiments.

(A) Multiplicity of infection (MOI) screen to optimize AdV transduction efficiency. H9c2 cells were transduced with AdV-GFP in different MOIs. Transduction efficiency was determined with an inverted fluorescence microscope (Axio Observer Z1, Zeiss). Optimal transduction efficiency was achieved with MOI 200 and 48 h of synthesis whereas higher MOIs increased apoptosis and lower MOIs yielded less protein. Scale bars represent 100 μ m. (B) To increase the MuRF1 protein amount for reliable SILAC-MS analysis 10 μ M MG132 was added for the last 6 – 8h of protein synthesis to inhibit UPS-dependent protein degradation. (C) Sample preparation for H9c2 SILAC-AP-MS experiments: after viral transduction MuRF proteins were synthesized for 48 h, AdV were washed away, cells were lysed, and subsequently APs were performed. After AP, respective samples were pooled and eluted.

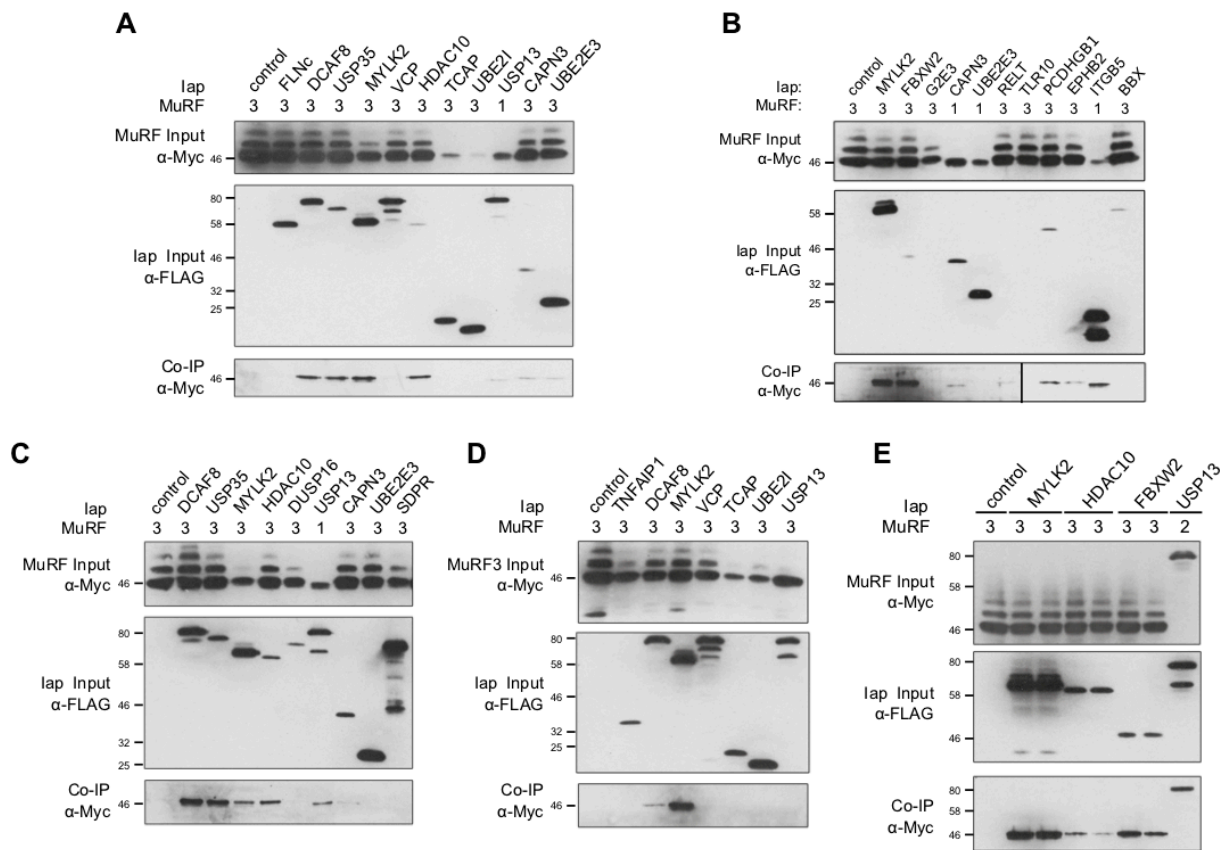


Fig. S3: Validation of MuRF protein-protein interactions.

Constructs for the expression of FLAG-tagged potential MuRF binding partners and for the indicated Myc(His)₆-tagged MuRF proteins were co-transfected into COS-7 cells. The FLAG-tagged proteins were immuno-precipitated and 14 candidates co-precipitated individual MuRF proteins (cf. Fig. 1 & Table S3 for a complete list of validated interaction partners). α -Myc-R IP samples in (B) were separated on two different SDS-gels, but are derived from the same experiment, were developed on the same films with the identical exposure times.

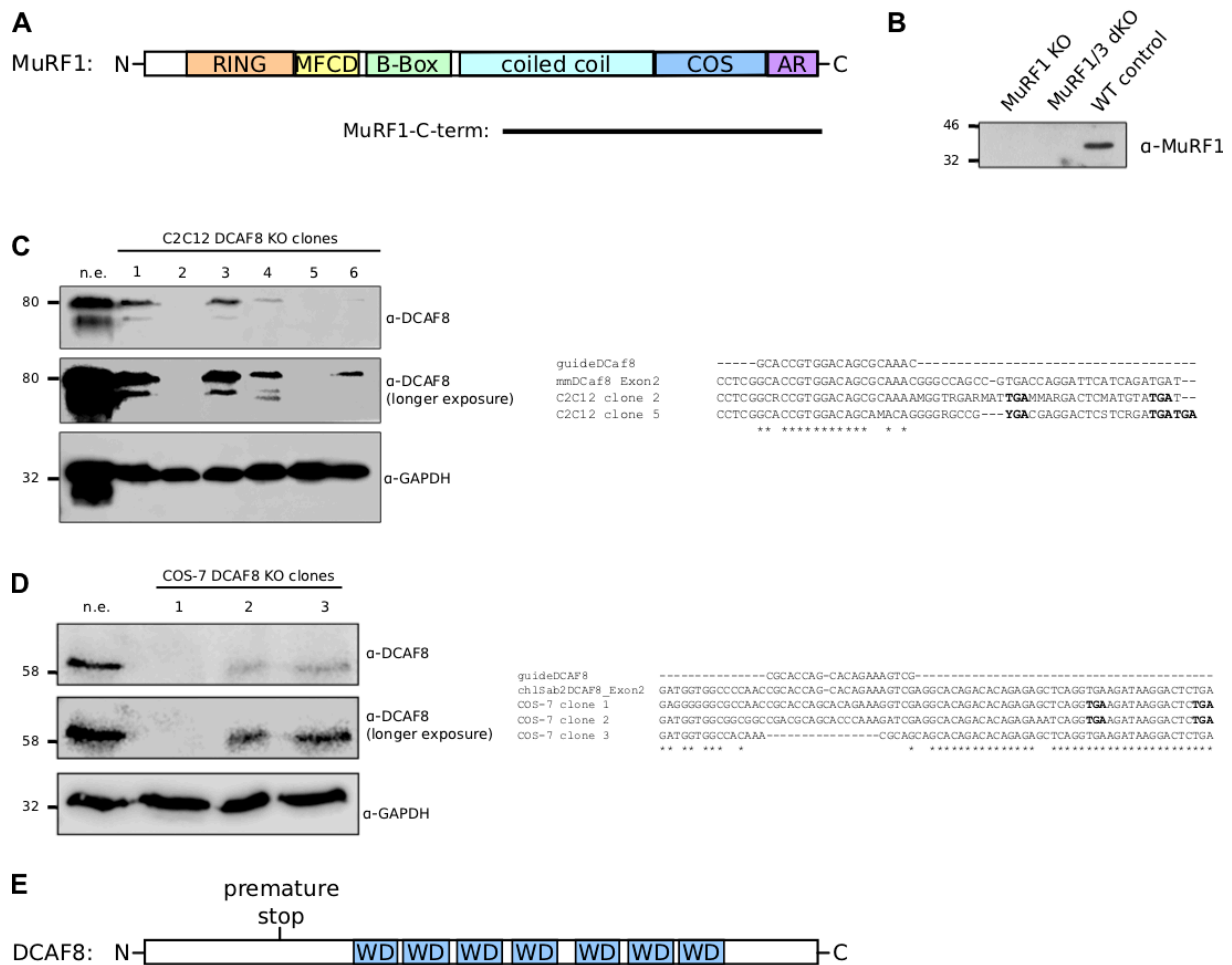


Fig. S4: Generation of a polyclonal MuRF1 specific antibody and C2C12 DCAF8 KO cells. (A) To generate a MuRF1 specific antibody, we cloned a C-terminal *Mus musculus* MuRF1 cDNA fragment (MuRF1-C-term: aa 185-355) into pGEX-6P-1. After expression and purification from *E. coli*, this peptide was used to produce the antibody in rabbits.. (B) To test the specificity of the anti-MuRF1 antibody, muscle tissue lysates from MuRF1 KO, MuRF1/MuRF3 double KO, and WT mice were analyzed by immunoblotting using this antibody. A specific MuRF1 signal was only detected in WT but not in KO or double KO mice. (C & D) Validation of the DCAF8 KO in C2C12 and COS-7 cells. left: Individual clones were analyzed for a stable DCAF8 KO via immunoblotting (n.e.: not edited control cells). right: Sequencing of the corresponding genomic region confirms the DCAF8 KO via introduction of premature stop codons in clones #2 and #5 for C2C12 cells and clone #1 for COS-7 cells (Bold: premature stop codons). C2C12 Δ DCAF8 Clone #5 was used throughout this study. (E) DCAF8 contains seven WD repeats, which are essential for substrate binding. However, the premature stop codon introduced into the C2C12 and COS-7 genes of DCAF8 results in loss of all WD domains rendering the truncated gene product non-functional.

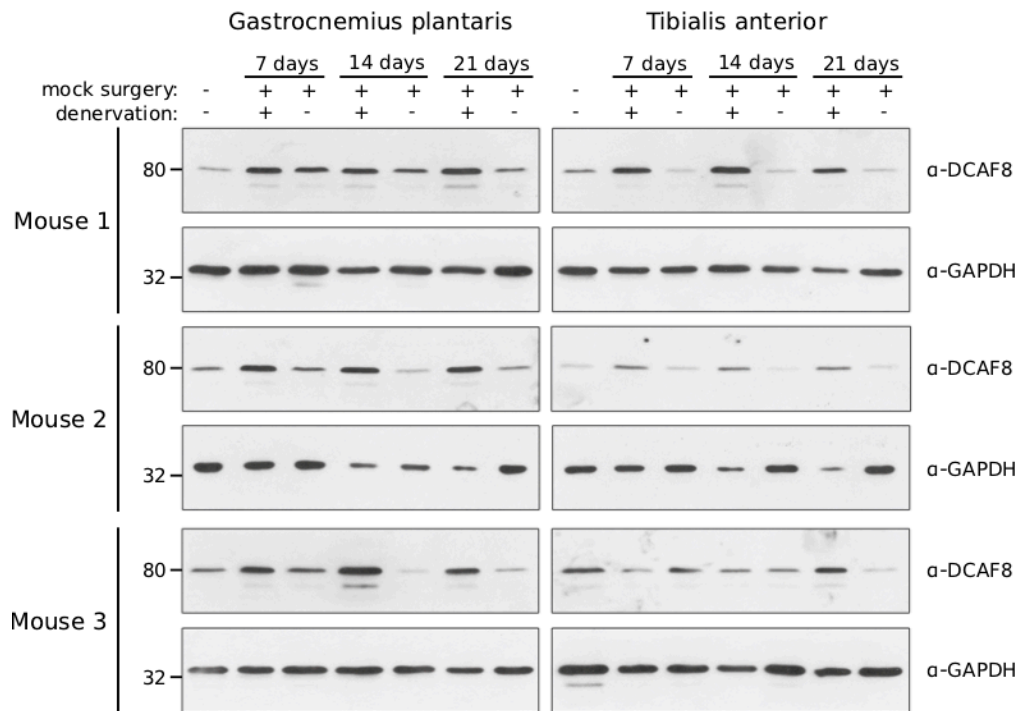


Fig. S5: DCAF8 is up-regulated after denervation-induced skeletal muscle atrophy in mice.

Skeletal muscle atrophy was induced by cutting the left sciatic nerve of C57BL/6N mice legs (for 7, 14, and 21 d). Contra-lateral legs and sham animals were used as controls. Subsequently GP and TA muscles were removed, lyzed, and equal protein amounts were analyzed with SDS-PAGE and immunoblotting using a specific DCAF8 antibody. DCAF8 protein amount strongly increased after 7, 14, and 21 d after denervation compared to operated and sham controls within GP and TA muscles.

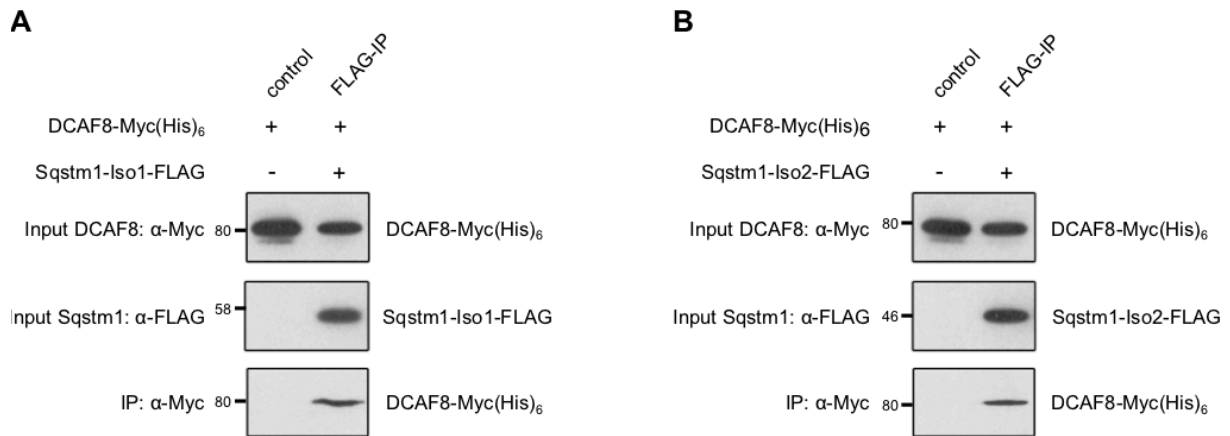


Fig. S6: DCAF8 interacts with Sqstm1/p62.

Sqstm1/p62 is a known MuRF1 interaction partner also up-regulated under muscle atrophy. Therefore, we wanted to check if Sqstm1/p62 might interact with DCAF8, too. Hence, two Sqstm1/p62-FLAG isoforms and DCAF8-Myc(His)₆ were synthesized for 48 h in COS-7 cells. Subsequently Sqstm1/p62-FLAG isoforms were precipitated, which revealed that both isoforms interact with DCAF8-Myc(His)₆.

Supplemental Tables

Table S1

Y2H auto-activation test results. Depicted are the auto-activation test results and the number of identified hits with the different N- or C-terminal truncated cDNA domain constructs used as baits in Y2H screenings. Abbr. Cc: Coiled coil, AR: Acidic rich, RING: Really Interesting New Gene, MFCD: MuRF-family-conserved domain.

Screen	Auto-activation	Positive clones
MuRF1-full length	+	-
MuRF1-cc-AR	+	-
MuRF1-RING-MFCD-B-Box	-	224
MuRF1-RING-MFCD	-	174
MuRF1-MFCD-B-box	-	184
MuRF2-full length	+	-
MuRF2-cc-AR	+	-
MuRF2-RING-MFCD-B-Box	-	251
MuRF2-RING-MFCD	-	224
MuRF2-MFCD-B-Box	-	167
MuRF3-full length	-	78
MuRF3-cc-AR	-	32

Table S2

Overview of the SILAC-AP-MS results. Depicted are the number of total identified proteins as well as proteins that have an H/L Ratio higher than 1.5.

Screen	Proteins	H/L Ratio \geq 1.5
MuRF1 Screen 1	781	131
MuRF1 Screen 2	827	98
MuRF2 Screen 1	833	35
MuRF2 Screen 2	818	37
MuRF3 Screen 1	238	15
MuRF3 Screen 2	408	29

Table S3

Y2H screening results of all MuRF1 and MuRF2 bait domains tested.

[Click here to Download Table S3](#)

Table S4

Y2H screening results of MuRF3 full length bait.

[Click here to Download Table S4](#)

Table S5

Y2H screening results of MuRF3 coiled coil domain bait.

[Click here to Download Table S5](#)

Table S6

Y2H screening results of unspecific MuRF3 binders.

[Click here to Download Table S6](#)

Table S7

Results from the 1st MuRF1 SILAC-AP-MS screen.

[Click here to Download Table S7](#)

Table S8

Results from the 2nd MuRF1 SILAC-AP-MS screen.

[Click here to Download Table S8](#)

Table S9

Results from the 1st MuRF2 SILAC-AP-MS screen.

[Click here to Download Table S9](#)

Table S10

Results from the 2nd MuRF2 SILAC-AP-MS screen.

[Click here to Download Table S10](#)

Table S11

Results from the 1st MuRF3 SILAC-AP-MS screen.

[Click here to Download Table S11](#)

Table S12

Results from the 2nd MuRF3 SILAC-AP-MS screen.

[Click here to Download Table S12](#)

Table S13

Data comparison of all performed screens.

[Click here to Download Table S13](#)

Table S14

Summary of conducted Co-IP experiments to validate the initial screen results. Co-IP experiments were carried out as described (see methods). Performed validation experiments are depicted with a PLUS or MINUS sign for interactions that could or could not be validated, respectively.

Protein	Validated Interaction		
	MuRF1	MuRF2	MuRF3
BBX			-
CAPN3	+		+
DCAF8	+	-	+
DUSP16			-
EPHB2			+
FBXW2			+
FLNC			-
G2E3			-
HDAC10			+
HNRNPLL	+		
ITGB5	+		
MICAL2	-		
MYLK2	+	+	+
NEDD8	+		
PCDHGB1			+
RELT			-
SDPR			-
Sqstm1/p62 isoform 1	+		
Sqstm1/p62 isoform 2	-		
TCAP			-
TLR10			-
TNFAIP1			-
UBE2E3	-		+
UBE2I			-
USP13	+	+	-
USP35	+	+	+
VCP			-

Table S15

Relative FLAG-MyHC protein content of COS-7 CHX assay. All samples were co-transfected with FLAG-MyHC. Relative data normalized to FLAG-MyHC content at the beginning of CHX treatment (100 µg/ml). Data represents the mean and standard error of at least 4 independent experiments.

Sample	Rel. FLAG-MyHC protein content [%]	
	0 min CHX	30 min CHX
COS-7 WT + FLAG-Cas9	100.00 ± 7.72 %	70.04 ± 2.72 %
COS-7 ΔDCAF8 + FLAG-Cas9	100.00 ± 4.36 %	96.23 ± 9.94 %
COS-7 ΔDCAF8 + MuRF1-Myc(His) ₆	100.00 ± 11.04 %	77.52 ± 5.33 %
COS-7 ΔDCAF8 + DCAF8-FLAG	100.00 ± 78.70%	60.96 ± 6.15 %

Table S16

Relative steady state FLAG-MyHC protein content in COS-7 cells. All samples were co-transfected with FLAG-MyHC. Relative data normalized to WT sample co-transfected with FLAG-Cas9 and FLAG-MyHC. Mean data and standard error of at least 4 independent experiments.

Sample	Rel. FLAG-MyHC protein content [%]	
	COS-7 WT	COS-7 ΔDCAF8
+ FLAG-Cas9	100.00 ± 4.54 %	224.39 ± 4.07
+ MuRF1-Myc(His) ₆	21.98 ± 4.70	142.81 ± 11.00
+ DCAF8-FLAG	n.a.	144.01 ± 6.41
+ MuRF1-Myc(His) ₆ & DCAF8-FLAG	n.a.	32.92 ± 5.27
+ MuRF1-Myc(His) ₆ & DCAF8-FLAG + 5 μM Lactacystin	94.45 ± 3.57	160.83 ± 4.43
+ MuRF1-Myc(His) ₆ & DCAF8-FLAG + 1 μM MLN4924	108.53 ± 12.53	81.43 ± 2.47